MYLONITIZATION OF THE WANAPITEI QUARTZITE, SUDBURY, ONTARIO.

MYLONITIZATION OF THE WANAPITEI QUARTZITE, SUDBURY, ONTARIO.

by

LEE ALLAN BAKER

A Research Paper

Submitted to the Department of Geology

in Partial Fulfillment of the Requirements

for the Degree

Bachelor of Science

McMaster University

April, 1978.

BACHELOR OF SCIENCE (1978) McMaster University
(Geology) Hamilton, Ontario.

TITLE: MYLONITIZATION OF THE WANAPITEI QUARTZITE, SUDBURY, ONTARIO.

AUTHOR: Lee Allan Baker

SUPERVISOR: Dr. P.M. Clifford

NUMBER OF PAGES: viii, 54

SCOPE AND CONTENTS:

Mylonitized Wanapitei quartzite (Huronian-aged), was examined in detail at two occurrences along the Grenville front near Sudbury, Ontario.

In the Coniston study area, the rocks show an increase in mylonitization from crush breccia to ultramylonite as the Wanapitei fault is approached.

The prevalence of optically observed features such as undulatory extinction, subgrain development and deformation lamellae increases with the mylonitization. The occurrence of these features can be explained in terms of dislocation movements within the quartz crystal lattice.

The mylonites were produced by pure shear or simple shear since on the deformation plot the samples lie between constriction-type deformation and flattening-type deformation with a $\overline{k} = 0.985$.

Dislocation climb and glide were the dominant deformation mechanisms operating in these rocks. However, as the grain size is reduced Nabarro-Herring creep may have become a dominant mechanism of the matrix of the mylonites.

ACKNOWLEDGEMENTS

The writer is especially grateful to Dr. P.M. Clifford for his suggestion and supervision of the research. Thanks are also extended to Dr. H.D. Grundy for his assistance in regard to the X-ray diffraction techniques and the interpretation of the results. The following are thanked for their assistance: Mr. L. Zwicker for preparing the thin sections; Mr. F. Pearson and F. Smith for their aid with S.E.M. techniques; and Mr. J. Whorwood for his assistance in regard to all photographic aspects of this report. Thanks are also extended to Mrs. J. Gallo for typing and proof-reading the manuscript.

TABLE OF CONTENTS

LIST OF FIGURES

LIST OF PLATES

LIST OF TABLES

CHAPTER I

INTRODUCTION

In the vicinity of Sudbury, Ontario, Huronian metasedimentary rocks, mainly quartzites, are sandwiched between the Grenville Province of highly metamorphosed rocks to the southeast and the Southern Province of less metamorphosed rocks to the northwest. The "Grenville Front" marks the transition between Grenville and Southern province rocks and in the Sudbury area is characterized by a zone of intensely cataclasized and more commonly, mylonitized rocks. A "mylonite" is a coherent microscopic pressure-breccia that possesses a definite fluxion structure or cataclastic foliation. A cataclasite or microbreccia on the other hand, is "a severely deformed microscopic pressure-breccia that does not show a pronounced fluxion structure" (Higgins, 1971).

This report is concerned with the study of the mylonites along the Grenville front near Sudbury, Ontario, and the interpretation of the microscopic deformation mechanisms that caused their formation.

LOCATION OF STUDY

The areas of study lie immediately to the east and southeast of Sudbury, Ontario, near the village of Coniston in Neelon Township and along Highway 69 in Dill Township, respectively (Figure 1). Both areas are readily accessible by major roads.

The Coniston smelter of the International Nickel Company of Canada is the main landmark in the easternmost study area. Smelter fumes have almost completely destroyed the forest cover throughout most of the area; subsequent soil erosion has produced complete exposure of rock outcrops. The result is a somewhat desolate landscape with ridges of black gabbro and well-bedded quartzite rising above valleys in which soil erosion is well pronounced. The topography reflects the type of bedrock and demonstrates very well the geologic structure.

Both study areas are associated with the so-called Grenville Front, a boundary between the Grenville Province of highly metamorphosed rocks in the southeast and the Southern province of less metamorphosed rocks on the northwest. This "front" runs roughly northwest from Lake Huron across Ontario and into the northwest portion of Quebec. In the immediate area of study, the front passes through Dill, Neelon and Dryden Townships.

The topographic pattern of the Grenville Province is quite different from that of the southern province and thus the line of junction or "Grenville Front" can be traced on air photographs (Figure 2). The abundance of rock exposures and their easy accessibility makes this area one of the prime localities for studying the geological relation-

Figure 1

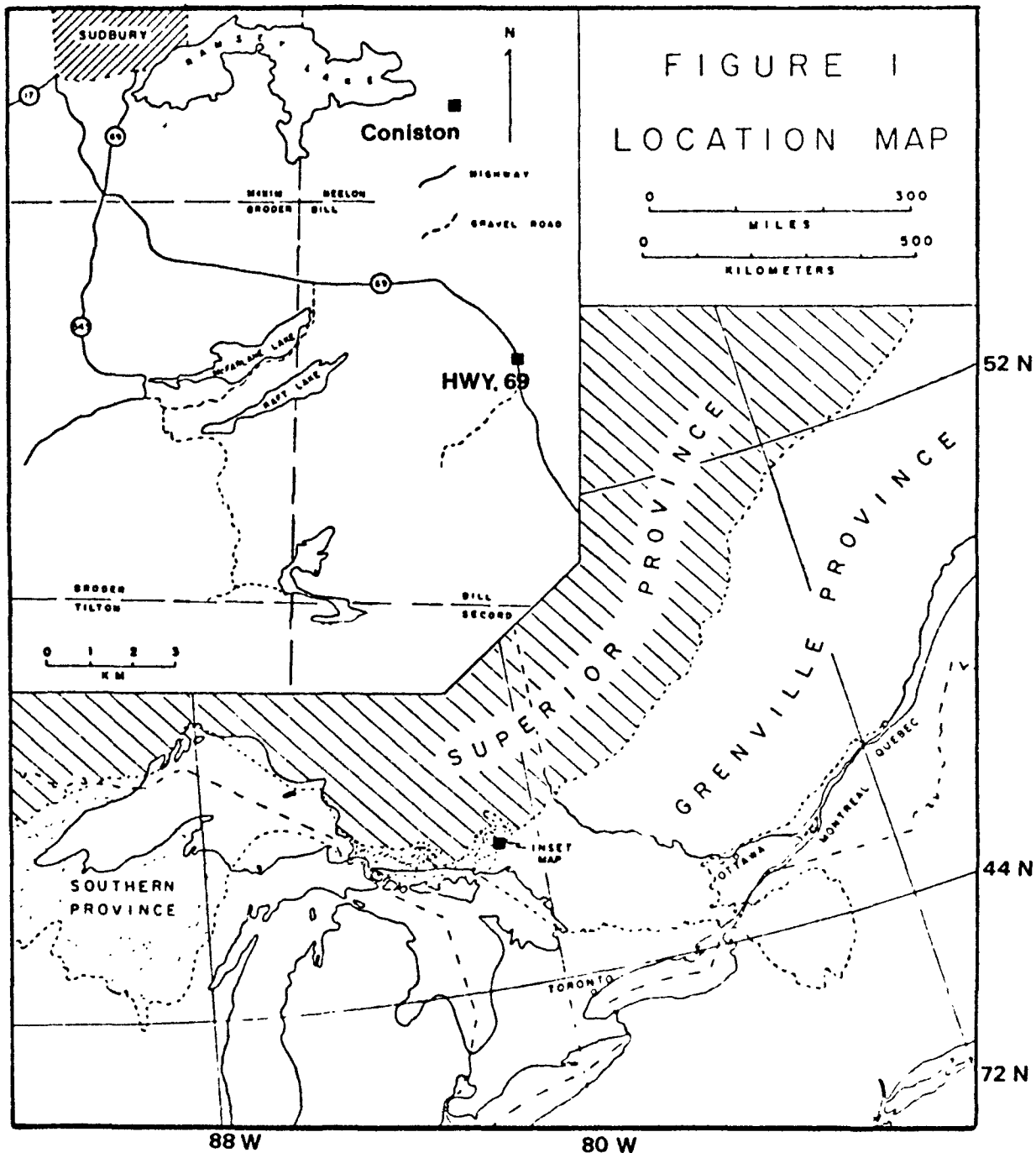

(modified from Hsu, 1968)

ships along the Grenville Front.

PREVIOUS WORK

Detailed geological investigations have been performed by Grant et al. (1962) in which they paid particular attention to defining the local lithologies and interpreting the structural history of the area. Petrology and geochemistry of the Highway 69 area is given by Kwak (1968, unpublished Ph.D. thesis). A structural analysis of the Grenville Front is outlined by Hsu (1968, unpublished M.Sc. thesis), and local rock nomenclature has been summarized by Henderson (1967).

GENERAL GEOLOGY

All the rocks in the two study areas are of Precambrian age. The Grenville Front marks the transition between deformed sedimentary rocks in the northwest and highly metamorphosed rocks to the southeast. Many theories have been put forth to explain the origin of the Front. Most commonly it is considered to be:

1. a metamorphic transition (Grant, 1962; Stockwell, 1964);
2. a fault (Johnston, 1954);
3. a combination of a metamorphic transition and a fault (Grant, 1964).

Southern Province Rocks

Immediately northwest of the Grenville Front near Sudbury are massive quartzites and subsidiary metagraywackes intruded by gabbro and "granite". The metasedimentary rocks are mostly Wanapitei (Mississagi)

quartzite with some graywacke. These rocks belong to the Sudbury group, which was thought to be pre-Huronian (Thomson, 1957), but is now recognized to be Huronian-aged (Card, 1968; Young and Church, 1966). Numerous small post-gabbro "granitic" bodies occurring close to the front were considered by Grant et al. (1962) to have resulted from the feldspathization of the Wanapitei quartzite. These granitic bodies were examined by this writer and were sampled at Baby Lake as granite-quartz monzonite where they show obvious intrusive characteristics (see Figure 2). In this area, the Wanapitei fault is observed as a quartz monzonite stockwork. Relatively underformed Wanapitei quartzite lies north of the fault and laminated to mylonitzed quartzite lies on the south side. Going southward, the laminated quartzite grades rapidly into feldspathic rock which forms the low hill through which the railway has been cut (see Plate 1). The strike of the Huronian metasediments in the Southern Province is generally east-west but in the vicinity of the Grenville Front, the strike swings to a northwest-southwest direction (Dalziel et al., 1969).

Grenville Province Rocks

Although Grenville Province rocks are highly variable in lithology they may be thought of as essentially amphibolites and gneisses ranging in composition from psammitic to pelitic. Intensive regional migmatization has resulted in the presence of numerous concordant pegmatitic foliae in both the gneisses and the amphibolites (Dalziel et al., 1969). Phemister (1961) and Grant et al. (1962) concluded that the gneisses and amphibolites southeast of the front near Sudbury are the equivalents of the Huronian metasediments and the Sudbury gabbros

FIGURE 2. Coniston sample locations and general geology.

LEGEND

Lithologic Units

1. Quartzite, laminated in some places.
2. Felspathic laminated quartzite with minor granitic intrusions.
3. Psammitic and pelitic gneisses and paragneisses.

Symbols

White numerals - sample locations

- Canadian Pacific Railway.
- position of Wanapitei fault
- position of Grenville Front.

SCALE

The scale is approximately 1:6700 or 1" to about 1/10 miles.

Figure 2

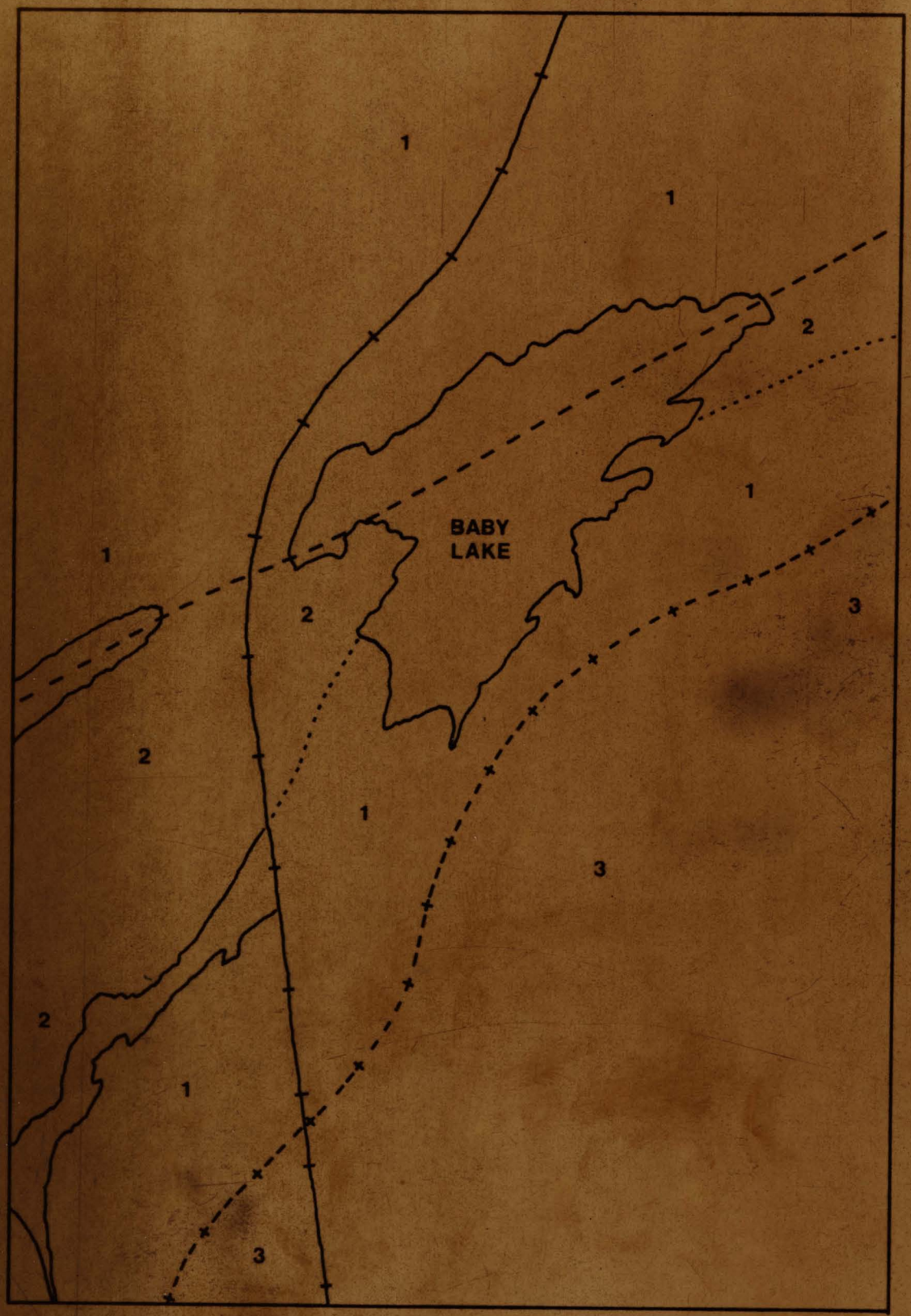

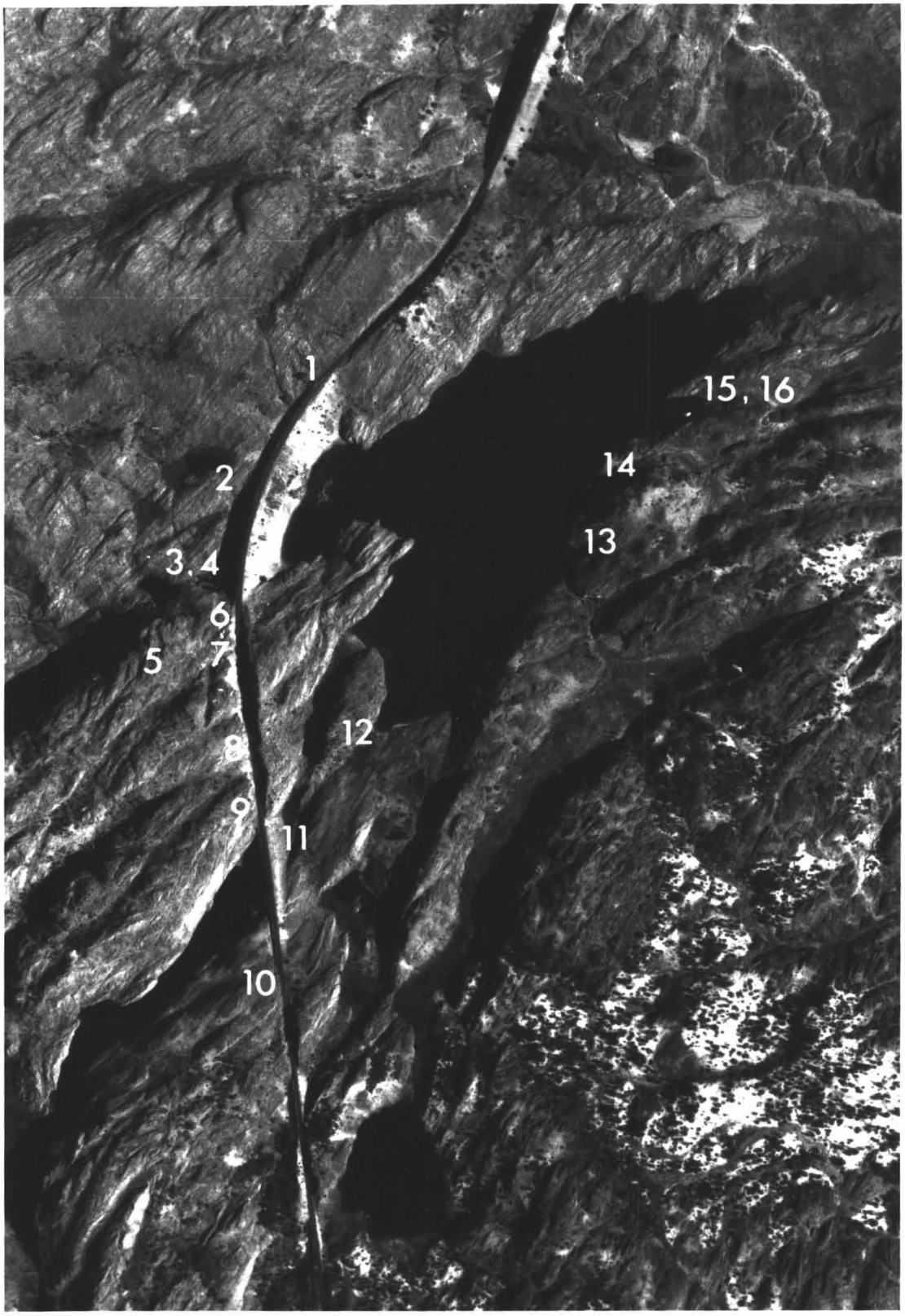
1
15, 16
14
2
13
3, 4
6
7
5
12
8
9
11
10

Figure 2

PLATE 1

(a) View looking westward along the strike of the Wanapitei fault from the Canadian Pacific Railroad toward Daisy Lake, Southern Neelon Township. The fault plane is near the middle of the photo and runs through the talus at the base of the ridge. The fault dips south (left) and is occupied by a quartz stockwork. Bedded Wanapitei quartzite lies to the right of the fault and feldspathic sedimentary rocks are on the left side.

(b) Mylonitized quartzite at the Highway 69 outcrop (sample #27).

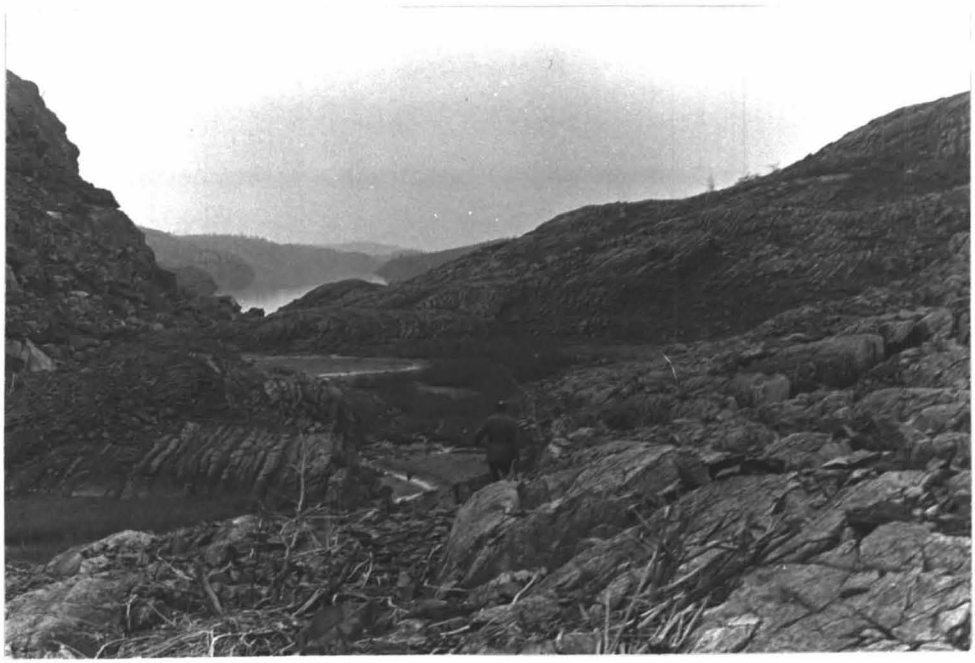

(a)

(b)

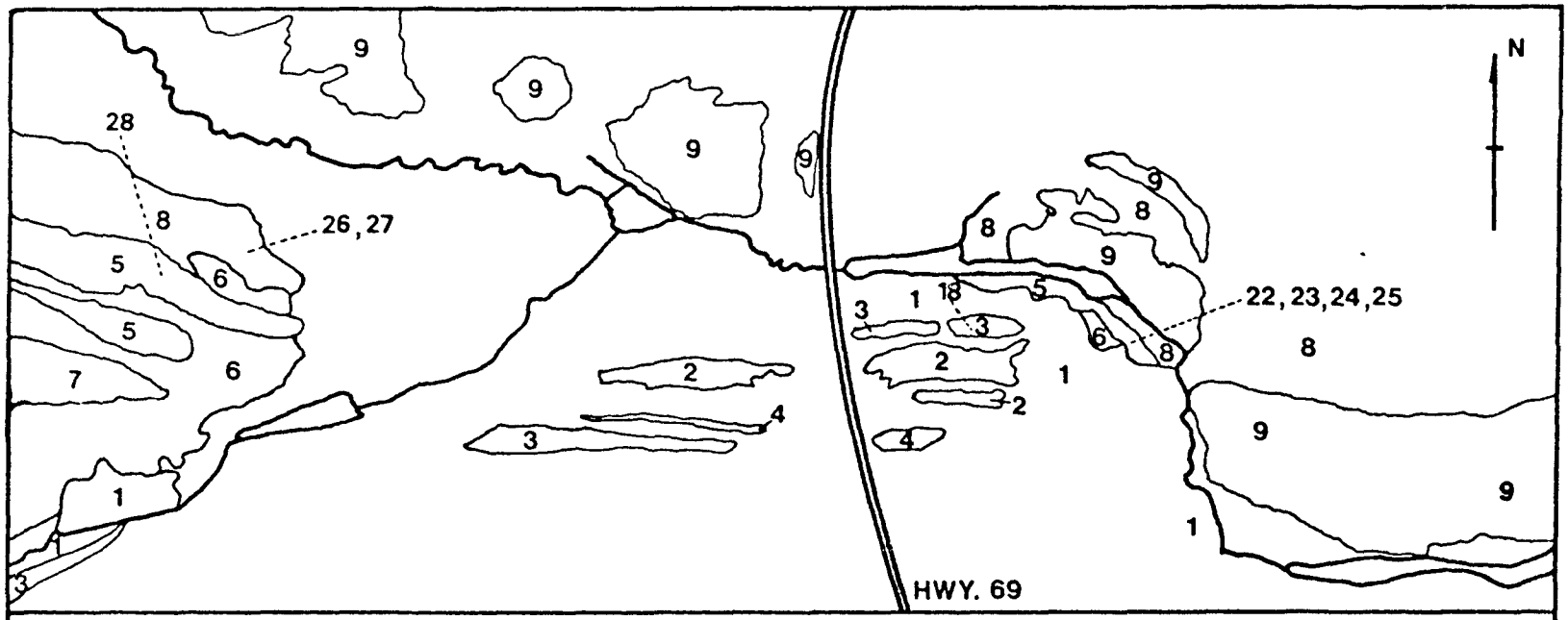

LEGEND

Grenville Province	Between Provinces	Southern Province	Map Symbols
1 gneiss	5 granite	8 quartzite	structural contact
2 biotite schist	6 K-felds.-ol.-gabbro	9 gabbro	geologic contact
3 amphibolite	7 olivine gabbro		
4 pegmatite			

Scale: 1:9700

Map showing HWY. 69 sample locations and regional geology in centre of Dill township.

(modified from Kwak, 1968)

Figure 3

PLATE 2

Severely kinked and folded Wanapitei quartzite at the Highway 69 study area. The outcrop is the origin of samples 22-24.

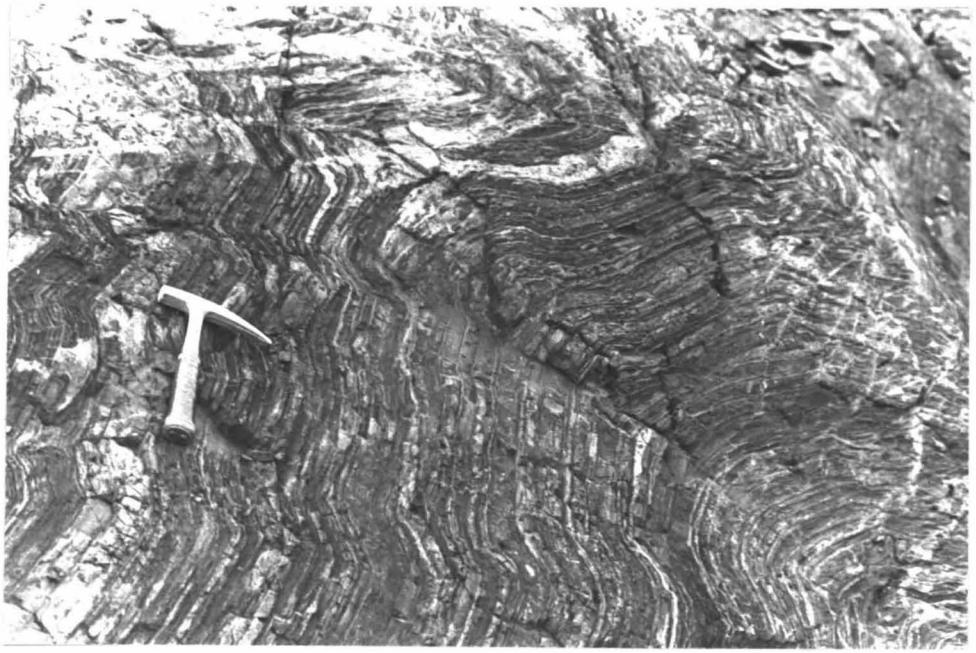

to the northwest. The Huronian sequence thickens to the southeast and certain horizons of the Mississagi quartzite (to part of which the Wanapitei is equivalent) are replaced by argillite. Card (1968) suggests that a gradual facies change could have been "telescoped" by subsequent tectonic activity in the vicinity of the front.

Grenville Front

The front is not a purely metamorphic transition as claimed by Phemister (1961) and Grant et al. (1962) because it is marked by a zone of intense mylonitization which affects both Southern and Grenville Province rocks. All the mylonitic rocks along this front are fine-grained, well-laminated and quartzitic. Dalziel et al. (1969) suggest that these rocks show varying degrees of recrystallization. The front may therefore be considered as a structural as well as a metamorphic transition, identified by a change in lithology from Southern Province Huronian metasediments to migmatitic Grenville Province gneisses. Segments of the front in the Sudbury area are characterized by intensely cataclasized and mylonitized quartzites.

LOCAL FAULTING

The largest fault in the area is the Wanapitei fault which is the easterly continuation of a great arcuate fault system, stretching a distance of about 150 miles (Grant et al., 1962). At certain places in the area, the rocks adjacent to the fault are crushed, brecciated and mylonitized to various degrees; at other locations, quartz veins and stockworks have been introduced along it. One of the best exposures of the fault is on the west side of Baby Lake where a quartz stockwork

fills the main break (Grant et al., 1962) (see Plate 1 and Figure 2).

Cooke (1946) has concluded that the Wanapitei fault is a thrust fault having a considerable component of movement in a dextral sense. The displacement along the fault has been estimated by Yates (1948) and by Grant et al. (1962) to be well over 5000 feet with the northside moving easterly.

SAMPLING LOCATIONS

Hand specimens were collected in both study areas as indicated by Figures 2 and 3. Brief descriptions of each sample are given in Table 1.

TABLE 1 HAND SPECIMEN DESCRIPTIONS

	SAMPLE	LITHOLOGY	ORIENTATION	COMMENTS
	LB-1	quartzite	034/80°E	platy, E-W cleavage 090/78°S
	LB-2	quartzite	069/62°S	undeformed?, felsic in parts
	LB-3	quartzite	051/75°S	somewhat deformed
	LB-4	quartzite	051/75°S	kink-folded mylonite
C	LB-5	quartzite	---	mylonite with conjugate kinks
O	LB-6	quartzite	076/56°S	mylonite
N	LB-7	granite?	137/31°E	felspathic mylonite?
I	LB-8	granite?	053/57°S	sample in massive outcrop
S	LB-9	quartz monzonite?	063/73°S	similar to LB-8
T	LB-10	quartzite	050/68°S	relic cross-beds in mylonite
O	LB-11	quartz melonite?	026/74°E	finely laminated mylonite
N	LB-12	quartz arenite?	058/72°S	kink-folded mylonite
	LB-13	mica-schist	068/58°S	flattened garnets and staurolite
	LB-14	granite?	---	mylonitized granite?
	LB-15	quartzite	088/52°S	mylonitized quartzite
	LB-16	quartzite	088/52°S	folded mylonitized quartzite
	LB-17	psammitic schist	060/64°S	finely laminated Grenville
H	LB-18	amphibolite	048/60°S	sheared, quartz-felspathic
I	LB-19	granite	076/32°S	prominent feldspar augen
G	LB-20	granite	071/45°S	lamination is secondary
H	LB-21	granite	095/36°S	occurs in "pod"
W	LB-22	quartzite?	075/39°S	kink-folded mylonite
A	LB-23	quartzite?	062/50°S	fine oblique lineation
Y	LB-24	quartzite?	062/50°S	feldspathic mylonite?
	LB-25	quartzite	078/56°S	kink-folded mylonite
6	LB-26	quartzite	055/59°S	appears glassy in parts
9	LB-27	quartzite	075/61°S	fine down-dip lineation
	LB-28	Granite	053/60°S	feldspar augen, deformed garnet

CHAPTER II

CHARACTERISTICS OF DEFORMATION

Analysis of the hand specimens indicates that the rocks adjacent to the Wanapitei fault have undergone varying degrees of deformation and in some cases the rocks have been classified as "mylonites". It is essential at this time to discuss cataclastic rocks and define several terms to be used throughout the remainder of this report.

Cataclastic Rocks

"Cataclastic rock" is a general term used to describe any rock produced by cataclasis. Cataclastic rocks can be divided into two main groups: (1) those without primary cohesion, and (2) those with primary cohesion. Fault breccia and fault gouge are examples of cataclastic rocks without primary cohesion. Cataclastic rocks with primary cohesion are metamorphic rocks which owe their cohesion to a combination of crystalloblastic and cataclastic processes (Higgins, 1971). These rocks can be further subdivided on the basis of whether or not they possess "fluxion structure", a cataclastic foliation. Rocks without fluxion structure are termed microbreccia or cataclasite. Rocks with a definite fluxion structure are termed protomylonite, mylonite and ultramylonite. The differentiation here is based on the proportion of matrix in the rock.

Cataclastic rocks can be best classified quantitatively by using the approximate size of the prophyroclasts and matrix combined with the approximate percentage of these features (see Table 2). Most mylonites show a bimodal distribution of grain sizes; the largest set of grains are termed "porphyroclasts" and the smaller set the "matrix". In general, matrix grains are one order of magnitude smaller than porphyroclasts.

* TABLE 2 CLASSIFICATION OF CATACLASTIC ROCKS

(Modified from Higgins, 1971)

<table>
<tr><td>Rocks Without Primary Cohesion</td><td colspan="7">Rocks with Primary Cohesion</td></tr>
<tr><td rowspan="4">Fault Breccia
> 30% Rock Fragments</td><td colspan="2">Nature of Matrix</td><td colspan="5">Proportion of Matrix</td></tr>
<tr><td rowspan="3">Crushed</td><td></td><td>0-10%</td><td>10-30%</td><td>30-50%</td><td>50-70%</td><td>70-90%</td><td>> 90%</td></tr>
<tr><td>Foliated</td><td rowspan="2">Crush or Micro-Breccia</td><td>Proto-mylonite "B"</td><td>Proto-mylonite "A"</td><td>Mylonite "B"</td><td>Mylonite "A"</td><td>Ultra-mylonite</td></tr>
<tr><td>Massive</td><td>Proto-cataclasite "B"</td><td>Proto-cataclasite "A"</td><td>Cataclasite "B"</td><td>Cataclasite "A"</td><td>Ultra-cataclasite</td></tr>
<tr><td rowspan="3">Fault Gouge
> 30% Rock Fragments</td><td rowspan="3">Recrystallized</td><td>Minor</td><td colspan="5">Hartschiefer</td></tr>
<tr><td>Major</td><td colspan="5">Blastomylonite</td></tr>
<tr><td>Glassy</td><td colspan="5">Pseudotachylite or Hyalomylonite</td></tr>
</table>

* Note: All categories are gradational.

DEFINITIONS

Crush breccia - An intensely fractured cohesive breccia in which the grains and fragments are without form orientation (Higgins, 1971).

Fault breccia - A rock composed of angular to rounded fragments formed by crushing or gringing along a fault. Most fragments are visible to the naked eye and comprise more than 30% of the rock. Coherence, if present, is due to secondary processes (Higgins, 1971).

Fault gouge - Pastelike rock material formed by crushing and grinding along a fault. Most individual fragments are too small to be visible to the naked eye, and any coherence present is due to secondary processes (Higgins, 1971).

Mylonite - The term "mylonite" (from the Greek mylon, a mill) was first introduced by Lapworth (1885) for "microscopic pressure breccias with fluxion structure, in which the interstitial dusty, siliceous and kaolinitic paste has only crystallized in part", the type specimens being found along the Moine thrust zone in Scotland. More recently, the word has come to mean "a coherent microscopic pressure breccia with fluxion structure which may be megascopic [sic] or visible only in thin section and with porphyroclasts about 0.2 mm in size. Mylonites generally show recrystallization and the formation of new minerals (neomineralization) but the dominant texture is cataclastic" (Higgins, 1971).

Further subdivision of the term mylonite is shown in Table 2.

Hartschiefer - A micro-brecciated rock with rigid parallel banding and a matrix affected by minor post-tectonic recrystallization independent of the layering. The recrystallization involves only the matrix portion of the rock (Spry, 1969).

Blastomylonite - A mylonite in which recrystallization is so pronounced that the original cataclastic texture can only be recognized with difficulty.

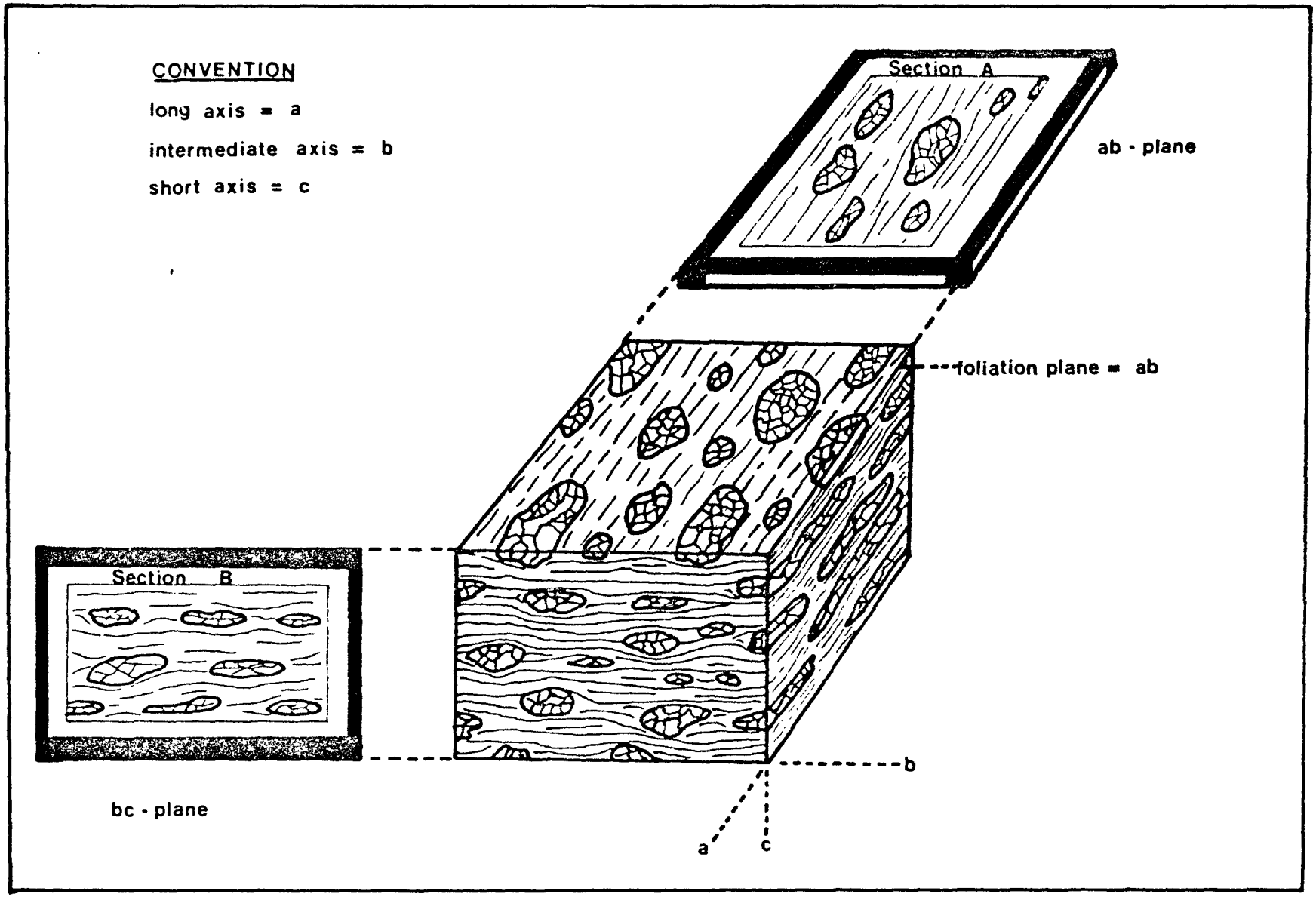

Schematic diagram showing main mylonite features, fabric axes orientation, and thin-section positions.

Figure 4

In a blastomylonite, both the matrix and prophyroclasts have been recrystallized (Spry, 1969).

Hyalomylonite or Pseudotachylyte - A mylonite containing glassy material produced by melting during deformation (Spry, 1969).

PETROLOGY

Two thin sections were cut from each hand specimen, one in the plane of the foliation (the ab plane) and one normal to the plane of foliation (the bc plane). This is diagramatically represented in Figure 4. The sections of each sample were examined using a Zeiss polarizing light microscope and the results are summarized in Table 3.

It is evidenced from Table 3 that as the fault is approached from either side, the degree of mylonitization of the rocks increases. As the degree of mylonitization increases, it is observed that there are:

Increases in	Decreases in
1. matrix proportion	1. porphyroclast grain sizes
2. fineness of matrix foliation	2. total number of porphyroclasts
3. "eyeing" of porphyroclasts	
4. degree of fracturing of porphyroclasts	
5. intensity of undulatory extinction	
6. ribbon structure in quartz, (coalescence of grains)	
7. sub-grain development	
8. deformation lamellae	

TABLE 3 PETROLOGIC OBSERVATIONS

SAMPLE #	MINERALOGICAL CLASSIFICATION	STRUCTURAL CLASSIFICATION	QUARTZ DEFORMATION FEATURES
		C O N I S T O N A R E A	
1	Quartzite	Protomylonite "B"	minor undulatory extinction
2	Quartzite	Crush breccia	minor undulatory extinction
3	Quartzite	Mylonite "B"	undulatory extinction, minor sub-graining
4	Quartzite	Mylonite "B"	undulatory extinction, pronounced sub-graining
	P O S I T I O N O F W A N A P I T E I F A U L T		
6	Quartzite	Ultramylonite	intense undulatory extinction and sub-graining, deformation lamellae and ribbon structure.
5	Quartzite	Mylonite "A"	intense undulatory extinction, sub-graining, minor deformation lamellae.
7	Granite?	Augen mylonite	minor undulatory extinction
15	Quartzite	Mylonite "A"	Undulatory extinction, sub-graining, minor deformation lamellae.
16	Quartzite	Mylonite "B"	Undulatory extinction, minor sub-graining
14	Quartzite	Protomylonite "B"	Undulatory extinction
8	Quartzite	Protomylonite "B"	Undulatory extinction
13	Mica-schist?	Protomylonite "B"	Undulatory extinction
12	Quartzite	Protomylonite "B"	Minor undulatory extinction
9	Granite?	Protocataclasite	Minor undulatory extinction
11	Quartzite	Protocataclasite	Minor undulatory extinction
10	Quartzite	Protomylonite "B"	Minor undulatory extinction
	H I G H W A Y 6 9 A R E A		
18	Quartzite	Mylonite "A"	Undulatory extinction, sub-graining
19	Quartzite	Protomylonite "A"	Undulatory extinction, minor sub-graining
20	Granite	Protomylonite "B"	Undulatory extinction
21	Granite	Protomylonite "A"	Undulatory extinction, minor sub-graining
22	Granite	Ultramylonite	Undulatory extinction, sub-graining, ribbon structure.
23	Quartzite	Ultramylonite	Undulatory extinction, sub-graining, ribbon structure.
24	Quartzite	Ultramylonite	Undulatory extinction, sub-graining, ribbon structure.
25	Quartzite	Mylonite "A"	Undulatory extinction, sub-graining
26	Quartzite	Mylonite "A"	Undulatory extinction, sub-graining
27	Quartzite	Mylonite "A"	Undulatory extinction, sub-graining
28	Granite	Protomylonite "B"	Minor undulatory extinction

NOTE: All rocks are gradational, samples are arranged with respect to distance from fault in the Coniston Area.

PLATE 3

(a) Sample 2B - Crush breccia. Note that there is no developed fluxion structure. The crushed matrix can be seen around and in between the larger quartz and feldspar porphyroclasts.

Magnification 25x.

(b) Sample 3B - Mylonite B. Note fluxion structure, and sub-graining in quartz porphyroclasts. Ribbon structure is beginning to form as the quartz porphyroclasts coalesce.

Magnification 25x.

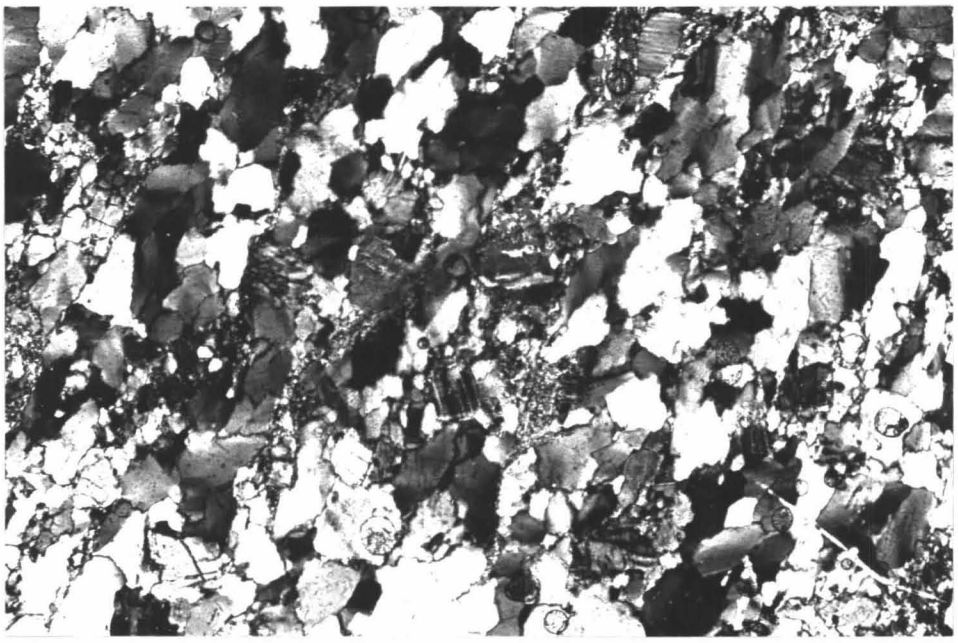

(a)

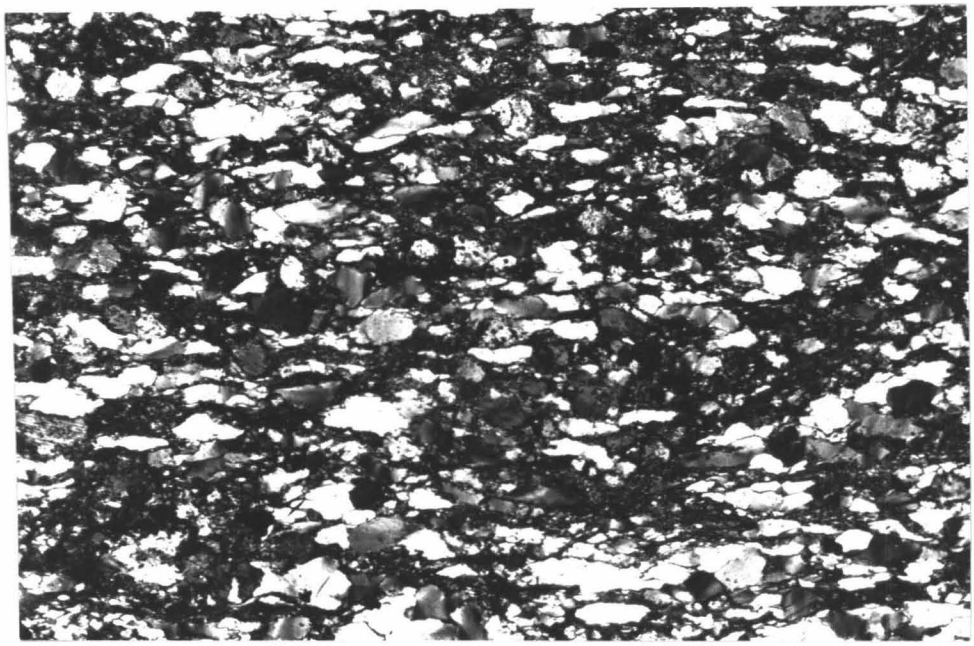

(b)

PLATE 4

(a) Sample 6B - Ultramylonite. Note the absence of large porphyroclasts and the ribbon structure developed in the quartz matrix. The fluxion structure is well-pronounced and some small recrystallized grains can be seen around the rims of the largest grains.

Magnification 25x.

(b) Sample 14 - Protomylonite B. Fluxion structure shown by dark band through centre of photo. Undulatory extinction and subgrain development can be seen in the quartz.

Magnification 25x.

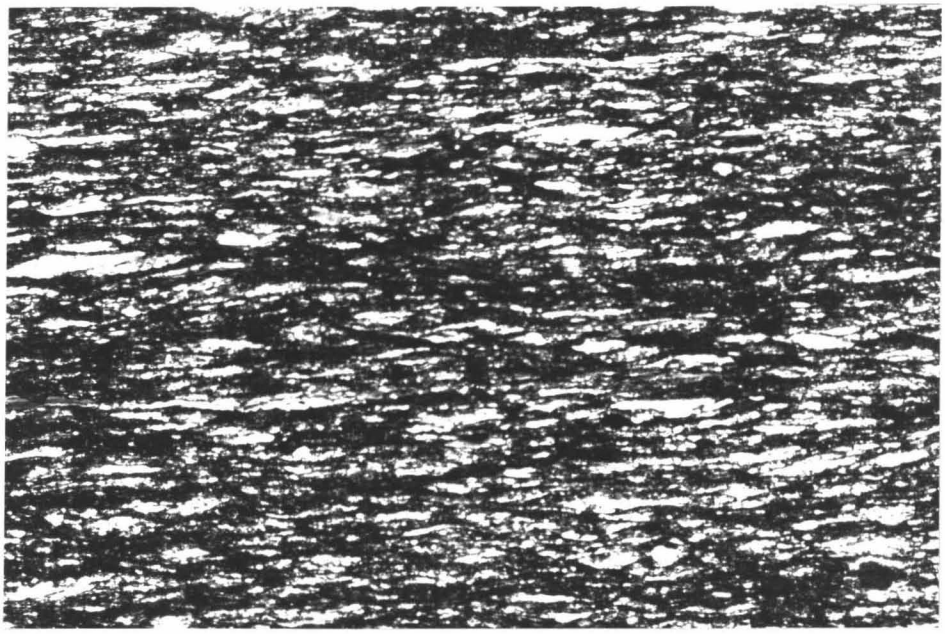

(a)

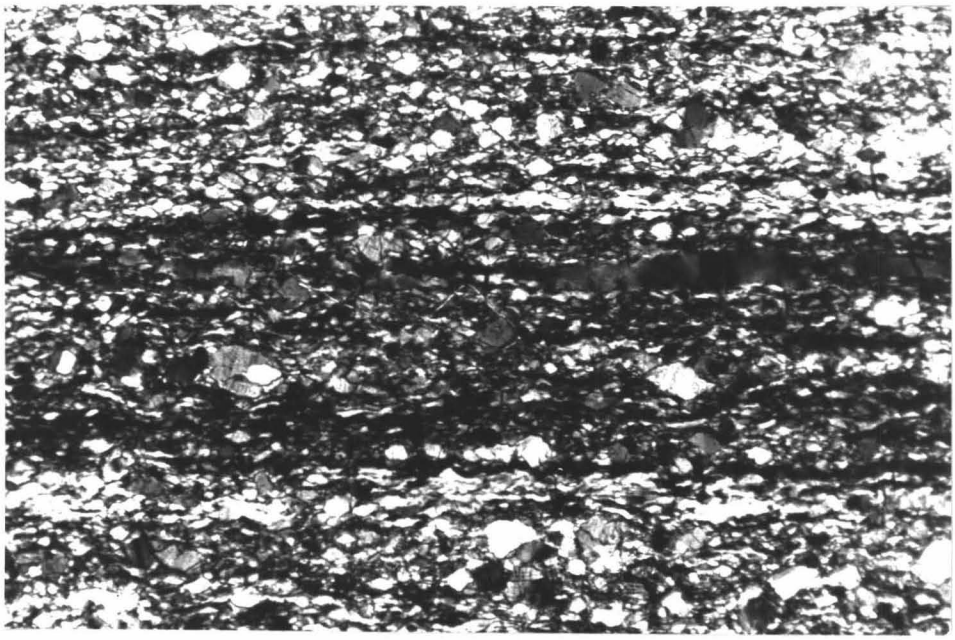

(b)

PLATE 5

(a) Sample 10B - Protomylonite "B". Note abundance of large quartz and feldspar porphroclasts and poorly developed fluxion structure.

Magnification 25x

(b) Sample 22B - Ultramylonite. Fluxion structure is shown by matrix, only 2 or 3 large porphyroclasts remain. In the upper right corner of the photo is a quartz-filled kink which is post-mylonitization.

Magnification 25x

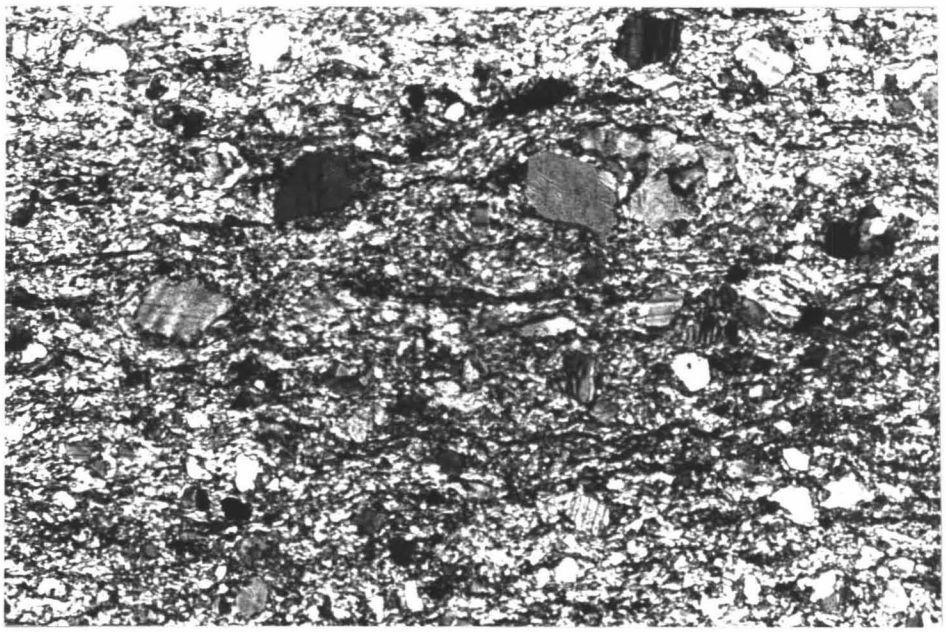

(a)

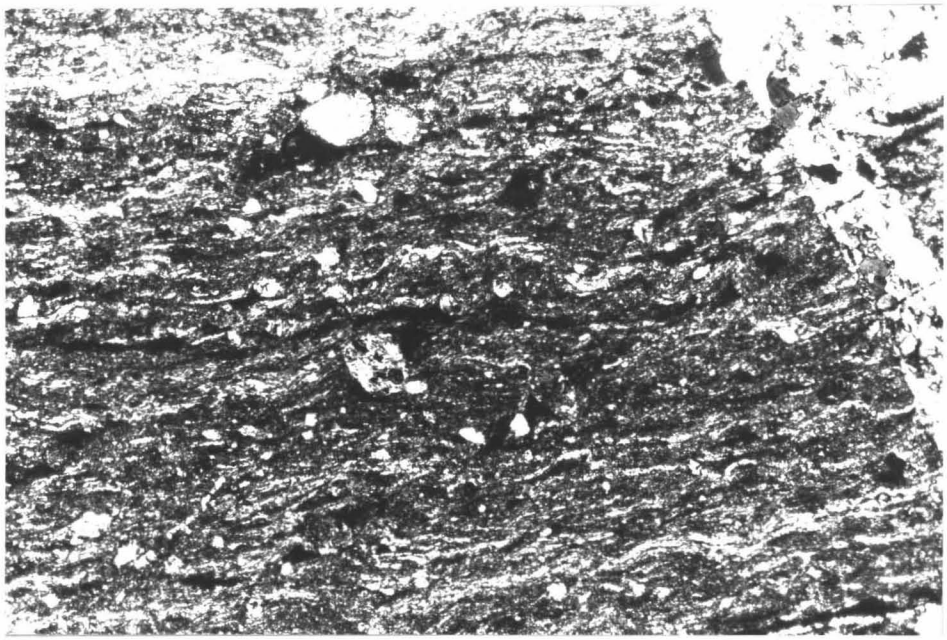

(b)

PLATE 6

Sample 25B - Mylonite "A". Fluxion structure is well-pronounced, recrystallized grains can be seen at the rims of the large porphyroclasts. These small grains show no deformation features.

Magnification 25x

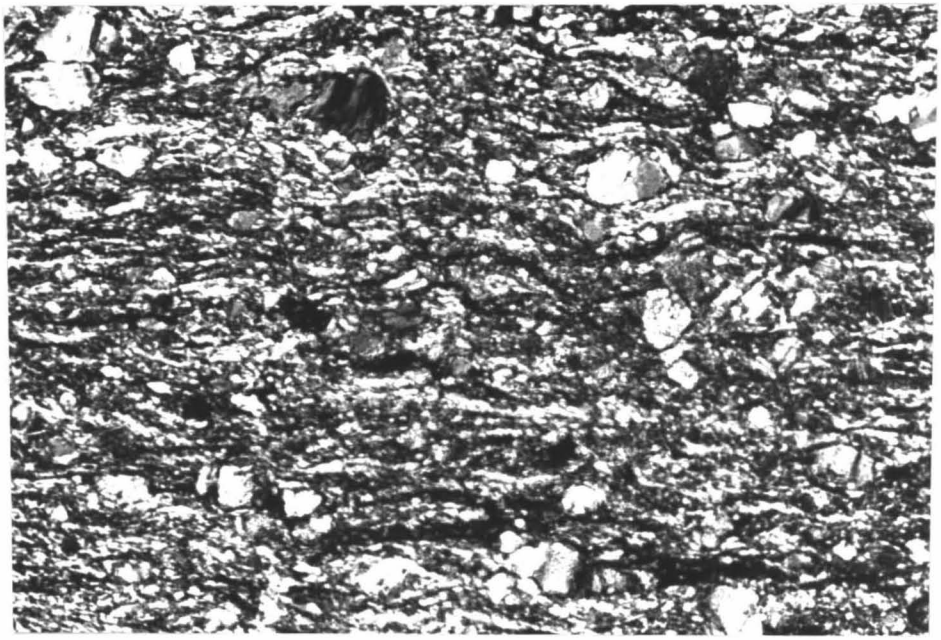

DEFORMATION PLOTS

Finite homogeneous strain is conveniently represented by the deformation ellipsoid. It is possible from studying the thin sections to determine directly the shape and orientation of the deformation ellipsoid for the rocks since the quartz and feldspar porphyroclasts are ellipsoids with their a and b axes measureable in thin section "A" and their b and c axes measureable in thin section "B".

The most suitable method of studying geometrical relationships among ellipsoids (porphyroclasts) is to plot the ratios of their axes on rectangular co-ordinates (Flinn, 1956). The ratios of $\frac{a}{b}$ and $\frac{b}{c}$ give the most convenient plot known as the deformation plot, where a is the longest axis of the porphyroclast, b the intermediate axis and c the shortest axis. Both ordinate and abscissa are positive in nature and each point on the plot represents a deformation ellipsoid characteristic of a particular sample.

When a rock deforms, an original sphere within it changes progressively through a series of ellipsoids varying continuously in shape until the deformation ceases. This type of deformation is known as "progressive deformation" (Flinn, 1962). The locus of the projections of these related ellipsoids on the deformation plot forms the deformation path. We may envisage stress-systems in rocks as being related to a series of ellipsoids on a deformation path. If the three principal stresses do not vary relatively to one another during deformation and the

stress-strain relationship is linear, then the deformation path will be a straight line radiating from the origin of the deformation plot (Flinn, 1962).

The deformation path is symbolized by k, where

$$k = \frac{(\frac{a}{b}) - 1}{(\frac{b}{c}) - 1}$$

for straight deformation paths (Flinn, 1962).

Figure 5 shows that $0 \leq k \leq \infty$; also, that $k = 0$ represents the path connecting all oblate (or in mineralogical terms, negative) uniaxial ellipsoids and $k = \infty$ all prolate (or positive) uniaxial ellipsoids. The diagonal of the plot $k = 1$, connects all ellipsoids in which the intermediate axis remains equal to the diameter of the original sphere. Ellipsoids such as this where $\Delta v = 0$, are produced by both pure shear and simple shear and it is this path defined by $k = 1$ that forms the boundary between constriction-type deformation ($1 < k \leq \infty$) and flattening-type deformation ($0 \leq k \leq 1$).

Determination of k

The best method for estimating k values is based on the direct measurement of the streaked-out quartz and feldspar porphyroclasts and matrix observed in the thin sections. These sections were cut both parallel and normal to the plane of foliation and were designated as sections "A" and "B", respectively (Figure 4). The axial ratios of 10-20 quartz porphyroclasts, feldspar porphyroclasts, and quartz grains in the matrix were measured in the sections that showed these features

Figure 5

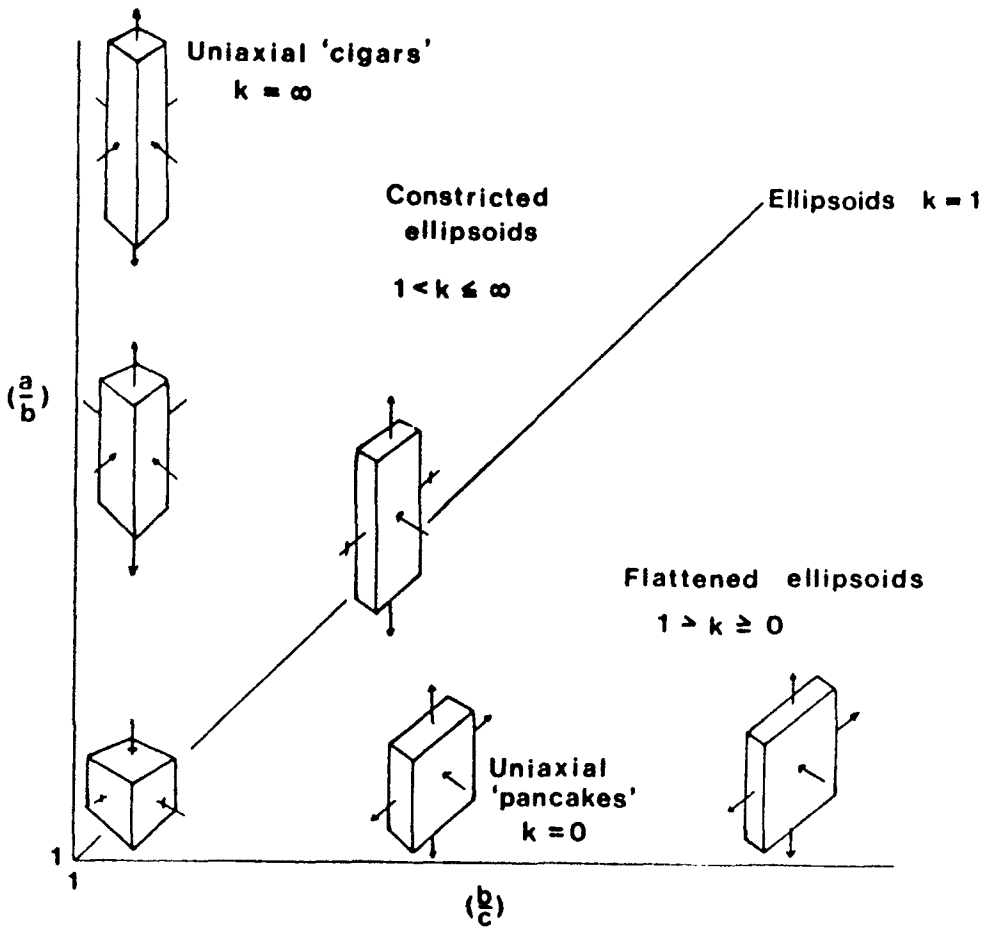

k = 0	uniaxial oblate
1 > k > 0	flattened
k = 1	plane – strain , $\Delta V = 0$
∞ > k > 1	constricted
k = ∞	uniaxial prolate

$$k = \frac{(\frac{a}{b}) - 1}{(\frac{b}{c}) - 1}$$

Graphical plot representing ellipsoids in terms of the ratios of the principal strains.

(after Flinn, 1962).

using a Shadomaster. (In many sections, the coalescence of porphyroblasts known texturally as ribboning, made the distinction of individual grains quite difficult.) Average axial ratios were then computed for each rock and the corresponding k value was determined from the formula.

Table 4 summarizes the axial ratios and k values determined for each quartzite sample. The standard deviation for k was determined by the formula

$$S^2 = \frac{\Sigma(k_i - \bar{k})^2}{N-1}$$

where S is the standard deviation,

k_i is k value for sample i,

$\bar{k}$ is the mean k value for N samples, and

N is the number of samples.

A summary of these computations is given in Table 5. The deformation plot for the Wanapitei quartzite is given in Figure 6.

X-RAY DIFFRACTION

Basic Theory

The phenomenon of X-ray diffraction by crystals results from a scattering process in which the X-rays are scattered by the electrons of the atoms without any change in wavelength. A diffracted beam is produced by such scattering only when certain geometrical conditions are satisfied, usually expressed in terms of the Bragg Law. The resulting diffraction pattern of a crystal, comprising both positions and intensities of the diffraction effects, is a fundamental physical property of the sub-

TABLE 4 QUARTZ PORPHYROCLAST DEFORMATION

SAMPLE #	STRUCTURAL CLASSIFICATION	$\frac{a}{b}$	$\frac{b}{c}$	k
1	Protomylonite "B"	2.25	2.5	.833
2	Crush breccia	1.26	1.1	2.6
3	Mylonite "B"	2.74	2.72	1.01
4	Mylonite "B"	3.78	3.58	1.08
POSITION OF WANAPITEI FAULT				
6	Ultramylonite	1.46	1.32	1.44
5	Mylonite "A"	1.63	1.57	1.1
7	Augen mylonite	----	----	----
15	Mylonite "A"	1.33	1.53	.622
16	Mylonite "B"	1.30	1.48	.625
14	Protomylonite "B"	1.34	1.63	.539
8	Protomylonite "B"	2.2	1.82	1.46
13	Protomylonite "B"	----	----	----
12	Protomylonite "B"	1.23	1.64	.359
9	Protocataclasite	----	----	----
11	Protocataclasite	1.52	1.47	1.10
10	Protomylonite "B"	1.25	1.65	.384
18	Mylonite "A"	1.43	1.72	.597
22	Ultramylonite	1.55	1.30	1.83
23	Ultramylonite	1.70	1.70	1.00
24	Ultramylonite	1.43	1.67	.64
25	Mylonite "A"	1.60	1.71	.845
26	Mylonite "A"	1.40	1.63	.635
27	Mylonite "A"	1.48	1.66	.727
28	Protocataclasite	----	----	----
FELDSPAR PORPHYROCLAST DEFORMATION				
1	Protomylonite "B"	1.31	1.19	1.105
2	Crush breccia	1.21	1.23	.913
10	Protomylonite "B"	1.34	1.28	1.214
QUARTZ MATRIX DEFORMATION				
1	Protomylonite "B"	3.04	2.82	1.12
3	Mylonite "B"	3.57	3.70	.952
4	Mylonite "B"	5.04	4.82	1.057
6	Ultramylonite	----	----	----
8	Protomylonite "B"	4.00	4.27	.917
11	Protocataclasite	4.58	4.75	.954
12	Protomylonite "B"	4.47	4.75	.925
27	Mylonite "A"	4.58	4.61	.992

TABLE 5 STANDARD DEVIATION OF k

TYPE OF DEFORMATION	$\bar{k}$	STANDARD DEVIATION
Quartz porphyroclast	.972	.543
Feldspar porphyroclast	1.07	.152
Quartz matrix	.984	.070

NOTE: $\bar{k}$ for quartz and feldspar porphyroclasts and quartz matrix is 0.985.

Figure 6

Deformation plot for Wanapitei quartzite at Coniston and HWY. 69

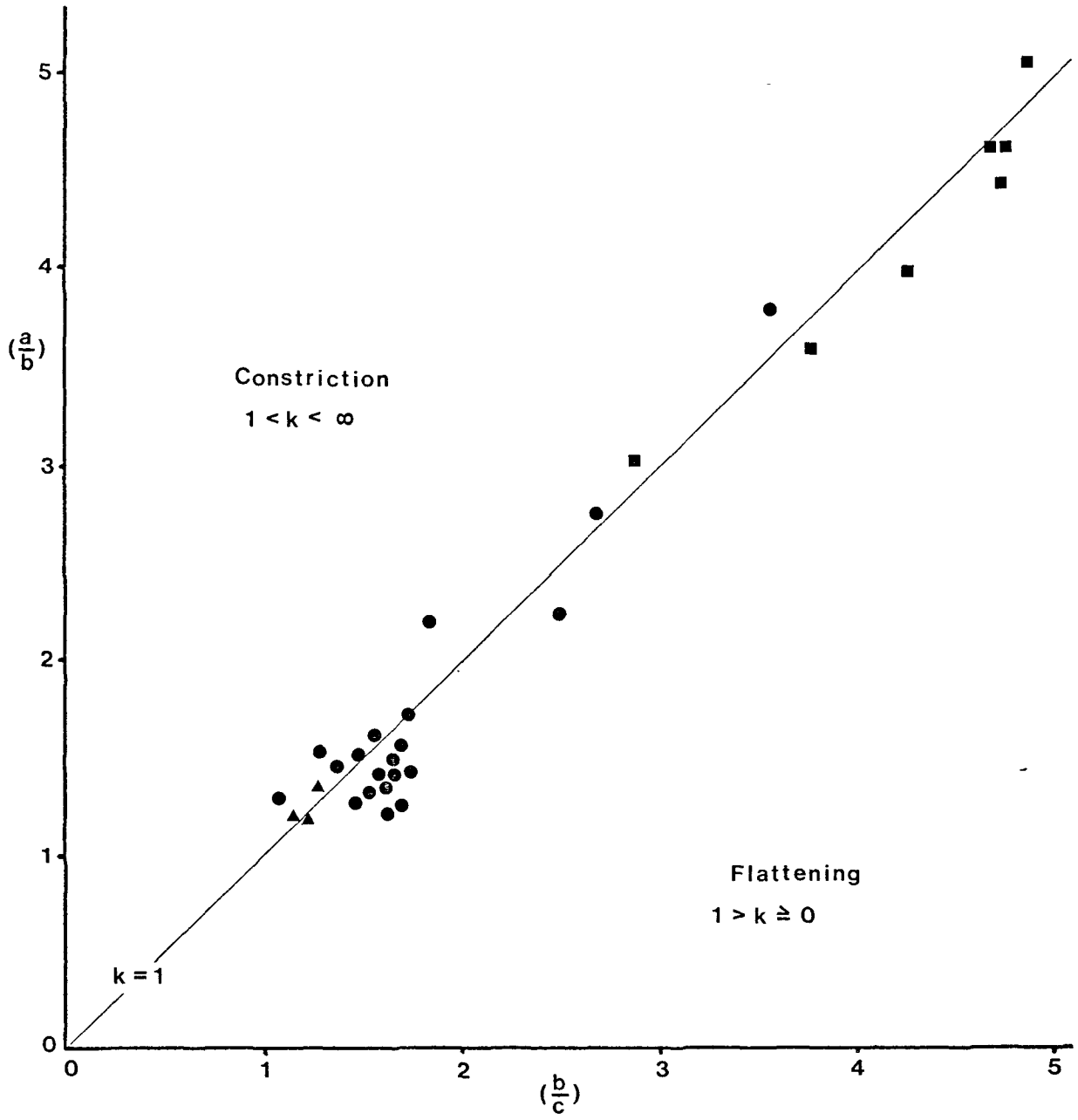

● – quartzite porphyroblast deformation

■ – quartzite matrix deformation

▲ – feldspar porphyroblast deformation

stance (Klug and Alexander, 1954). Analysis of these positions and intensities leads to a knowledge of the orientation of the unit cell and the crystallographic planes within.

Procedure

Rock slabs were analyzed by X-ray diffraction to determine any preferred orientation of crystallographic planes within the specimens. The Wanapitei quartzite is essentially pure quartz and therefore its X-ray diffraction pattern shows little or no contamination from other silicate minerals, such as feldspars. This allows a direct comparison of diffraction patterns for the quartzites and the quartz standard used to calibrate the spectrometer.

The diffraction peaks of prime interest are the (100) and (101) peaks of quartz. (In the hexagonal system these planes are properly designated as $(10\bar{1}0)$ and $(10\bar{1}1)$ but for simplicity they will be referred to as (100) and (101) planes, respectively.)

Rock slabs from the Coniston area (dimension = 5 x 2 x 0.5 cm) cut both parallel and normal to the plane of foliation were irradiated and the peak intensities calculated as in Figure 7. Table 6 summarizes these calculations.

The ratios of peak intensities for both sections is plotted against sample location in Figure 8. This graphical presentation suggests that the (100) plane of quartz, which is parallel to the "C" crystallographic axis becomes more oriented in the plane of foliation as one approaches the fault from either direction. In contrast to this, the (101) plane becomes less oriented in the plane of foliation.

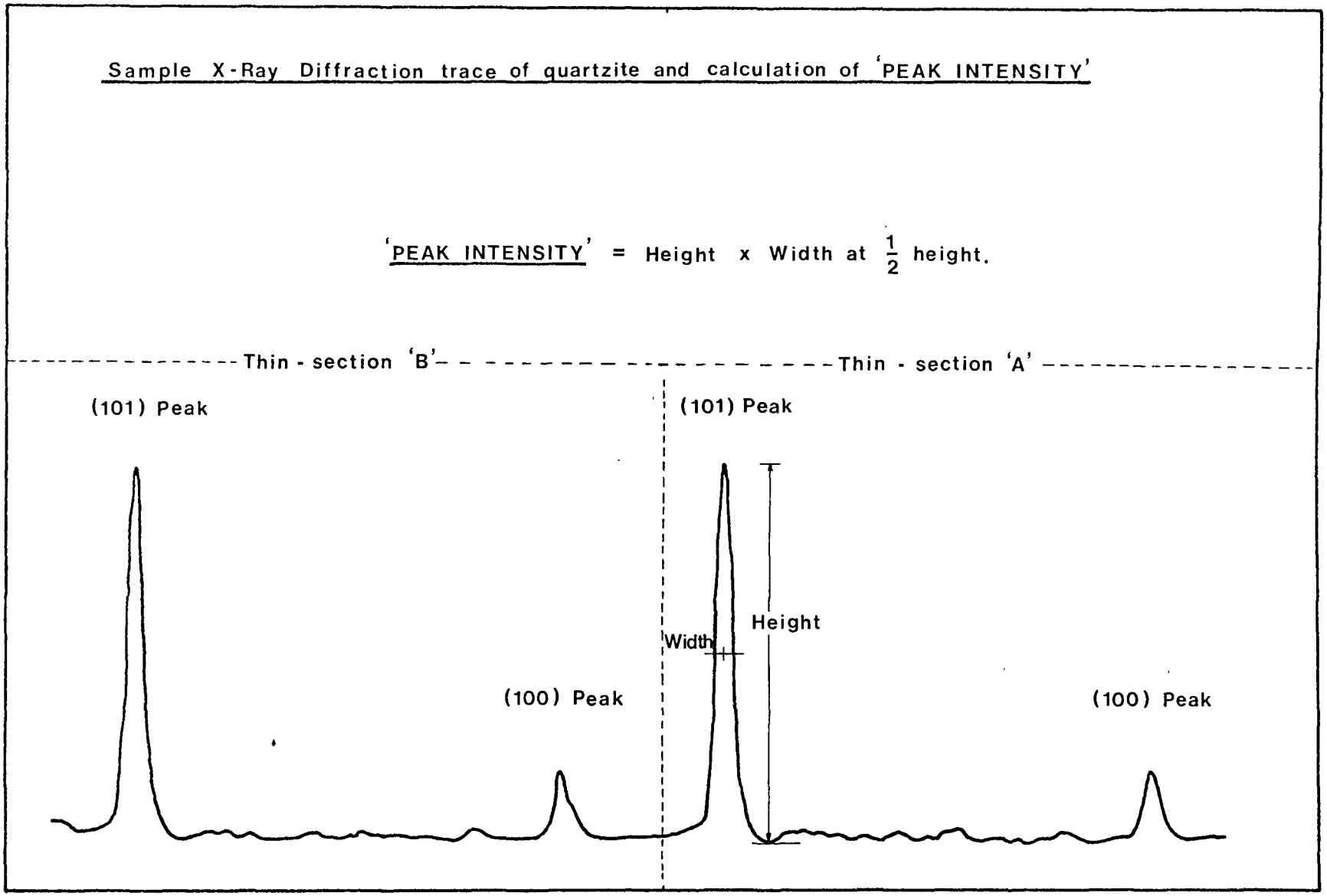
Sample X-Ray Diffraction trace of quartzite and calculation of 'PEAK INTENSITY'
'PEAK INTENSITY' = Height x Width at 1/2 height.
Thin - section 'B'
Thin - section 'A'
(101) Peak
(101) Peak
Width
Height
(100) Peak
(100) Peak

Figure 7

TABLE 6 X-RAY DIFFRACTION RESULTS

SAMPLE #	STRUCTURAL CLASSIFICATION	PEAK INTENSITY (100) SECTION "A"	PEAK INTENSITY (101) SECTION "A"	$(\frac{100}{101})$ SECTION "A"	PEAK INTENSITY (100) SECTION "B"	PEAK INTENSITY (101) SECTION "B"	$(\frac{100}{101})$ SECTION "B"
1	Protomylonite "B"	1.21	5.94	.200	1.00	5.30	.188
2	Crush breccia	1.74	7.55	.230	1.15	8.00	.144
3	Mylonite "B"	1.21	5.65	.214	1.08	6.97	.155
4	Mylonite "B"	1.37	5.45	.252	.664	4.93	.135
		P O S I T I O N O F W A N A P I T E I F A U L T					
6	Ultramylonite	1.025	3.46	.296	.600	5.03	.120
5	Mylonite "A"	1.41	4.40	.320	1.11	7.15	.155
15	Mylonite "A"	1.91	6.27	.305	.690	5.76	.120
16	Mylonite "B"	2.45	8.25	.296	1.45	9.5	.152
8	Protomylonite "B"	0.48	1.60	.300	.300	1.665	.180
12	Protomylonite "B"	1.32	4.80	.275	.101	4.50	.225
11	Protocataclasite	1.044	3.75	.278	.816	3.00	.272

Figure 8

Graph of PEAK INTENSITY RATIO vs. SAMPLE LOCATION for Coniston quartzites.

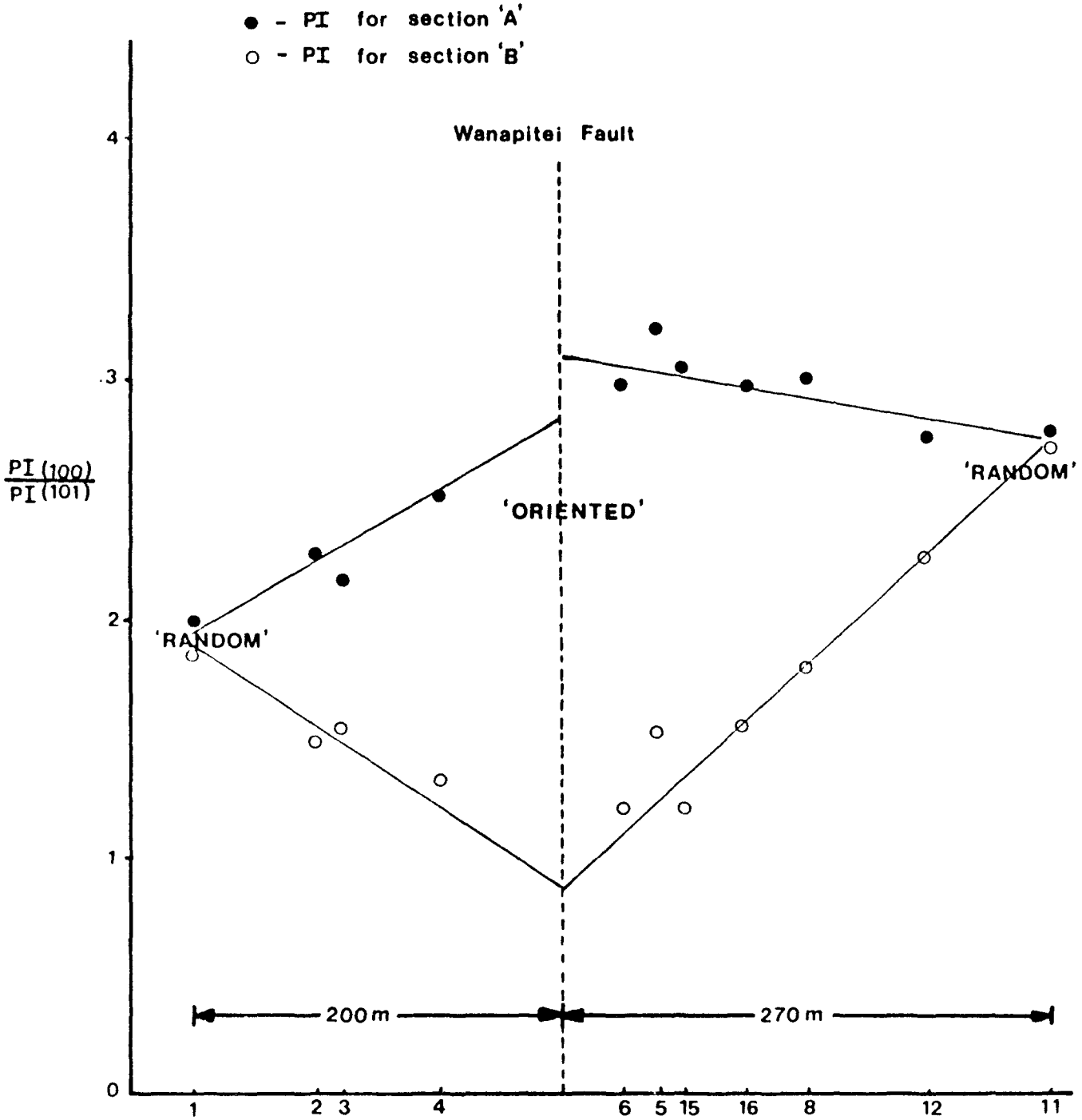

Approximately 200 m north and 270 m south of the fault, the degree of orientation of the (100) and (101) planes in both sections is essentially equal. It is at these points that the samples may be regarded as crystallographically random with respect to the orientation of the (100) and (101) planes.

SCANNING ELECTRON MICROSCOPE

Principle of Operation

The scanning electron microscope (SEM) employs a narrow beam of electrons which have been accelerated and brought to focus on the surface of a specimen. As the electron beam scans the surface, changes in composition, texture, or topography at the point where the electrons strike the specimen cause variations in the electron current and allow an image of the specimen to be formed on a viewing screen (Oatley, 1972). The resolution of the instrument can be of the order of a few tenths of a micron depending on the type of specimen and its preparation.

Analytical Procedure

Small rock chips of dimension 1 x 1 x 0.5 cm were cut perpendicular to the plane of foliation and coated with ^{14}C to increase the resolution. These samples were then analyzed with a Cambridge Stereoscan SEM and photomicrographs were taken of the observed deformation features. Although resolution was not possible down to the submicroscopic scale, the technique did provide photomicrographs of deformation on a fine scale. Some easily identified deformation features and mineralogical features are shown in the following micrographs, Plates 7 and 8.

PLATE 7

(a) Cataclastic shear zone in sample 10 - Protomylonite "B".

The quartz grains are intensely sheared and crushed in a line running from upper left to lower right in the photo. The magnification is 650x, the width of the sheared zone being about 100 μm. (Note: 1 micrometer (μm) = $\frac{1}{100}$ mm.)

(b) Undeformed quartz next to shear zone in sample 10 - Protomylonite "B".

The quartz grains are orthogonal and the shear zone begins in the upper right corner of the photo. The magnification is 2550x, the width of the photo being 28 μm.

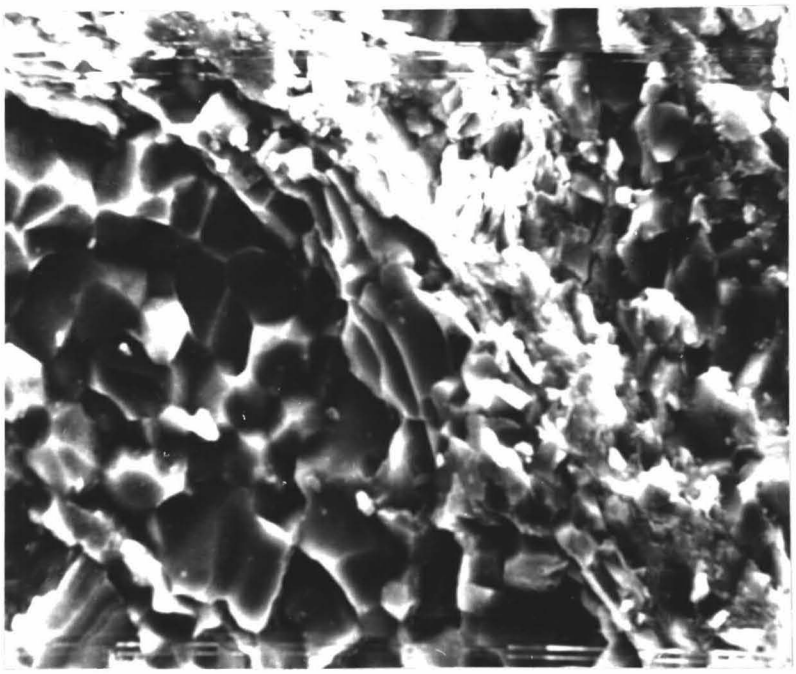

(a)

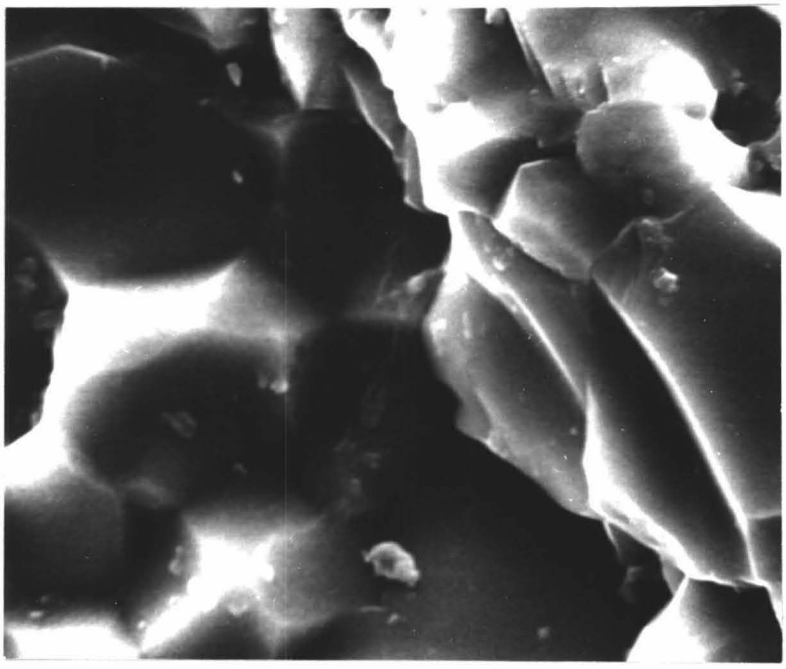

(b)

PLATE 8

(a) Sample 10 - Protomylonite "B". This photo shows the development and propagation of a microfracture in a quartz grain situation near the shear zone shown in plate 7 (a). Magnification is 1325x, the width of the photo is approximately 60 μm.

(b) Sample 4 - Mylonite "B". Note the separation of individual quartzitic layers, this occurring parallel to the plane of foliation in the rock. Magnification is 2650x. The width of the photo is approximately 30 μm.

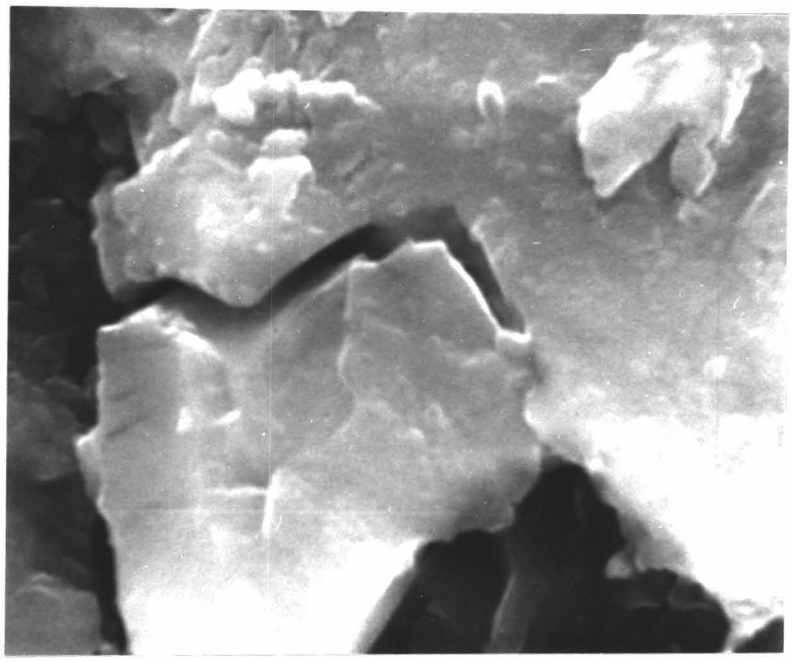

(a)

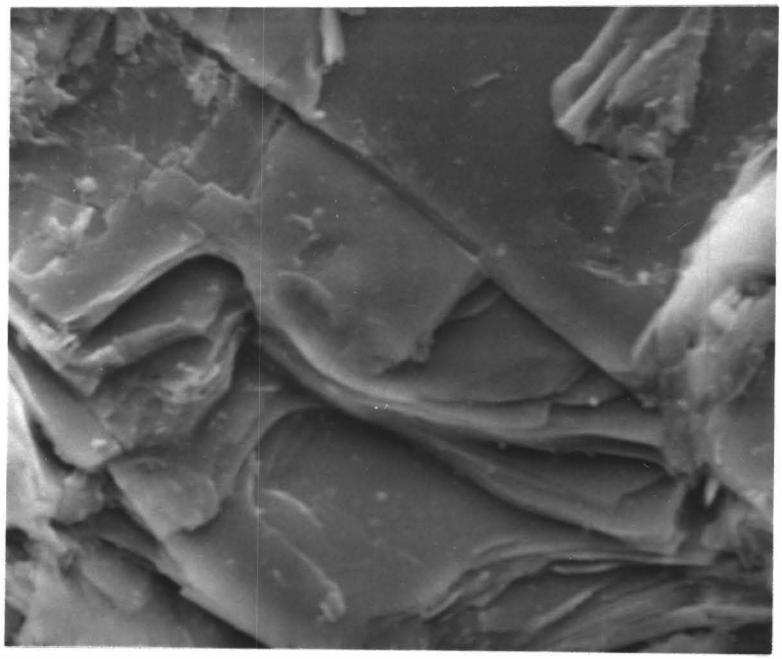

(b)

CHAPTER III

*MICROSCOPIC DEFORMATION MECHANISMS RESPONSIBLE FOR MYLONITE FORMATION

Introduction

The mechanisms and conditions involved in mylonite formation have been the source of much disagreement amongst experimental structural geologists. Most recent work suggests that there can be several possible mechanisms involved in the formation of a "mylonitic rock". Grain size reduction, the characteristic feature of mylonites, is observed to occur under high strain rates and low temperature conditions where the rocks are brittle and the deformation mechanism is principally microfracturing, or it can occur at high temperatures where the rocks behave in a ductile manner and the principle deformation mechanism is dislocation glide aided by recovery and recrystallization processes. Many workers such as Higgins (1971), Belliere (1971), and Krupicka and Sassano (1972) attribute the formation of mylonitic microstructures solely to brittle processes. It has since been suggested by others such as Bell and Ethridge (1973) and Tullis (1978) that brittle deformation is unnecessary for the formation of the typical mylonite and that microstructures such as undulatory extinction, subgrain development and deformation lamellae can be attributed to ductile deformation, recovery and recrystallization processes. Brittle deformation may contribute to the overall

---

* Reference for the discussion is: Tullis, J., Mylonites - Natural and Experimental, GSA short course, March, 1978. Boston, Massachusetts.

production of a mylonite but it need not be the dominant mechanism involved.

The following discussion will be concerned with brittle and ductile behaviour in rocks and how these processes relate to the observed microstructures found in mylonites.

BRITTLE vs. DUCTILE DEFORMATION IN ROCKS

Handin (1966) defines brittle deformation as having a very low permanent strain before a through-going fracture forms. In addition, there is an associated dicatancy or volume increase due to the opening up of microfractures (Paterson, 1970). In contrast to this, ductile behaviour involves independent finite strain, no through-going fracture formation, loss of cohesion or dilatancy (Paterson, 1969). Brittle behaviour is observed to occur at low pressures and temperatures whereas ductile behaviour occurs at higher temperatures and pressures. The general concensus amongst experimentalists according to Tullis (1978) is that brittle behaviour involves microfracturing whereas ductile behaviour involves microfracturing and in addition, sliding on fracture surfaces and grain boundaries.

MICROFRACTURING

When stress is applied to rock, many of the cracks and pores within the grains and along the grain boundaries will close. However, some cracks in favourable orientations will have local stress concentrations at the crack tips many times greater than the external applied stress and once they attain a certain size, they will propagate in a catastrophic manner. These cracks are oriented parallel to the maximum

compressive stress and low confining pressures and deviate up to 30° from the maximum compressive stress at higher confining pressures (Friedman, 1975). As the applied stress increases, new microfractures open faster than the old ones close and this produces the phenomenon of dilatancy, a volume increase (Brace et al., 1966). The microfractures form in a localized region and then propagate to form an intersecting en echelon network, producing a cataclastic zone. Samples deformed at lower pressures develop a single narrow fault zone since only a few cracks are nucleated prior to macroscopic failure. At high pressures, where cracks are in abundance, samples are observed to undergo a quasi-homogeneous deformation with no through-going faults which is termed by Borg et al. (1960) "cataclastic flow".

Experimentally deformed samples have been observed to contain arrays of microcracks and microgouge zones which can produce deformation bands, deformation lamellae and undulatory extinction, all of which are optically indistinguishable from those produced at higher temperatures by dislocation arrays (Tullis and Yund, 1977).

DISLOCATION GLIDE AND CLIMB

One may envisage dislocations as line imperfections which when stressed propagate through a crystal producing small offsets but not altering the crystal lattice in any fundamental way. Edge dislocations are regarded as an extra half-plane of material in the cubic lattice. All mineral grains within the rock contain dislocations which will move and allow new dislocations to form and move as the rock is stressed.

The "gliding" of dislocations is produced by external stresses and occurs along the most close-packed crystallographic planes. The process is enhanced by high temperatures since the increased thermal vibrations make it somewhat easier to break the bonds in the lattice. A dislocation can only propagate so far in that it will be pinned by other dislocations or lattice imperfections. This gives rise to the phenomenon of strain hardening, in which an increasing stress is required to produce each additional strain increment, since it takes higher stresses to force dislocations around or through obstacles. It is observed that at low temperatures, a small amount of dislocation glide may be followed by microfracturing and unavoidable failure of the rock. At higher temperatures, recovery and softening processes balance the strain hardening process and allow steady state deformation or "dislocation creep" to occur.

One of the principle recovery processes is "dislocation climb" which allows dislocations to climb over obstacles by shortening their extra half-planes. This process also permits dislocations to amalgamate into low energy stable walls, forming the observed microscopic feature known as subgrains. The development of subgrains was best developed close to the Wanapitei fault and in general, in rocks classed as ultramylonites. Therefore, the recovery process of dislocation climb must be a major process in rocks of this type.

Syntectonic recrystallization is another important recovery process active in the Sudbury mylonites. It involves the nucleation of small strain-free grains around the larger porphyroclasts, the process occurring at lower tempeatures and high stresses. Evidence for

recrystallization is given by the X-ray diffraction data which shows that as the fault is approached, there is an increase in the orientation of the (100) plane of quartz with respect to the (101) plane in the plane of foliation of the rock. This re-orientation as a response to stress can only be accomplished by recrystallization processes (H.D. Grundy, personal communication). High temperatures are not required to induce this process since re-orientation can occur when the crystal lattice is in a semi-solid to gel form, i.e., no actual melting need occur to facilitate the preferred orientation. In contrast to this, the samples far removed from the fault showed little or no preferred orientation of (100) with respect to (101) in the plane of foliation. Therefore, they probably did not undergo large amounts of recrystallization. In effect then, they may be envisaged as "crystallographically random" in which there would be equal chances of finding the (100) or (101) planes in the plane of foliation. Samples 1 and 10 in Figure 8 are regarded as crystallographically random.

Other optical evidence for dislocation glide includes deformation lamellae and undulatory extinction. Both of these features were best developed near the fault where mylonitization was greatest. This reinforces the suggestion that dislocation climb was a major recovery process near to the fault and in the mylonites in general.

The deformation lamellae may be regarded as simple dislocation arrays occurring in the mineral grains (White, 1973). Most undulatory extinction in metamorphic rocks is a bending of the lattice caused by excess dislocations of one sign. This is explained by the fact that quartz during low-medium grade metamorphism is in the α-phase field.

Since α-quartz is piezoelectric, not only will the individual grains be charged during deformation but also will the dislocations. Therefore, the predominance of dislocations of one sign is to be expected. As a result, the lattice will be systematically bent at each sub-grain wall and the net crystal effect is undulatory extinction (White, 1973).

VOLUME AND GRAIN BOUNDARY DIFFUSION

When a differential stress is applied to a rock, there is a tendency for the vacancies within the mineral grains to migrate toward the crystal boundaries that are perpendicular to the applied stress. As this happens, the material migrates toward the crystal boundaries that are perpendicular to the minimum applied stress. The process produces a steady state flow known as diffusion creep. Nabarro-Herring creep is the name given to diffusion that occurs through the volume of the grains and Coble creep if diffusion occurs along grain boundaries.

Stocker and Ashby (1973) suggest that if Nabarro-Herring creep occurs in nature, it would be in a high temperature and low stress regime. The presence of fluids within the rock enhances grain boundary diffusion and thus pressure solution when observed probably represents Coble creep. If this mechanism occurs during deformation, then there should be an absence of dislocation features such as deformation lamellae, undulatory extinction, and there should be no crystallographically preferred orientation. Since all of these features were noted in the Sudbury mylonites studied herein, then it is reasonable to assume that Coble creep was not a dominant mechanism responsible for their formation.

EFFECTS OF TEMPERATURE ON THE DEFORMATION MECHANISMS

Increasing temperature greatly enhances the generation and glide of dislocations and therefore, the transition from brittle to ductile deformation will decrease with increasing temperature. In the transition region, dislocations have a limited mobility and therefore cracks will be initiated due to dislocation pile-ups and entanglements. In this temperature zone which is generally about 0.5 Tm (Tm = melting point of rock), strong work hardening will occur and one will observe microfracture development primarily. At temperatures in the order of 0.75 Tm recovery processes become dominant and dislocation glide occurs without strain hardening. Therefore, steady state deformation (diffusion creep) can occur without the generation of a large number of new microfractures. At the high temperature end of this regime, syntectonic recrystallization will occur after very low strains. Finally, at very high temperatures, close to Tm diffusion creep or grain boundary sliding will become the dominant deformation mechanism provided the grain size is relatively small.

DEFORMATION MECHANISM MAPS

Attention should be drawn to the question of how the deformation mechanisms responsible for mylonite formation vary with different conditions such as temperature, grain size, strain rate and differential stress. The deformation mechanism map developed by Ashby (see Stocker and Ashby, 1973) and modified by White (1973) is one way of illustrating all the variety of possible deformation mechanisms and how they vary with different conditions. More importantly, it shows the different stress, temperature and grain size fields within which different mechanisms are dominant.

In order to construct a deformation mechanism map for the Sudbury mylonites that is at all meaningful, one must make several assumptions about the various conditions in the area at the time of mylonitization. These assumptions are as follows:

(1) Kwak (1968) has estimated the temperature of metamorphism in the area to be in the range of 475 to 725°C with corresponding pressures between 4.8 and 7.7 kilobars. It is reasonable to assume that the temperature of mylonitization was in this range, probably at the lower end. An estimate of 400-600°C would seem plausible. (It is observed in the diagram that the temperature of mylonitization has little bearing on what deformation mechanism will be dominant in the Sudbury mylonites, when all other parameters are considered.)

(2) The differential stress is estimated to be of the order of 100 bars (10.0 megapascals), giving a log ($\Delta\sigma$) of 2.0. Mantle values for $\Delta\sigma$ are estimated at 10-100 bars where the rocks behave in a ductile manner.

Crustal $\Delta\sigma$ values are estimated at 1000-3000 bars.

(3) The strain rate falls roughly between 10^{-8} and 10^{-14} per second. Time averaged strain rates along the San Andreas fault have been estimated at 10^{-14} per sec and in certain areas such as Hollister, California, the strain rate has been measured at 10^{-11} per sec, approximately (Geotimes, Nov., 1971, p. 33).

(4) The grain size of the mylonites is a petrographically measured feature and therefore is quite reliable. The largest porphyroblasts are about 1 mm in diameter and the matrix grains average 10 μm in size.

It is now possible to construct a deformation mechanism map which shows the dominant mechanisms acting over a wide range of conditions assumed for the Sudbury area. In addition, a "deformation mechanism tunnel" may be shown on the map which indicates the range of conditions over which mylonitization could have proceeded in order to produce the types of mylonites observed in the area. The deformation mechanism map is shown in Figure 9.

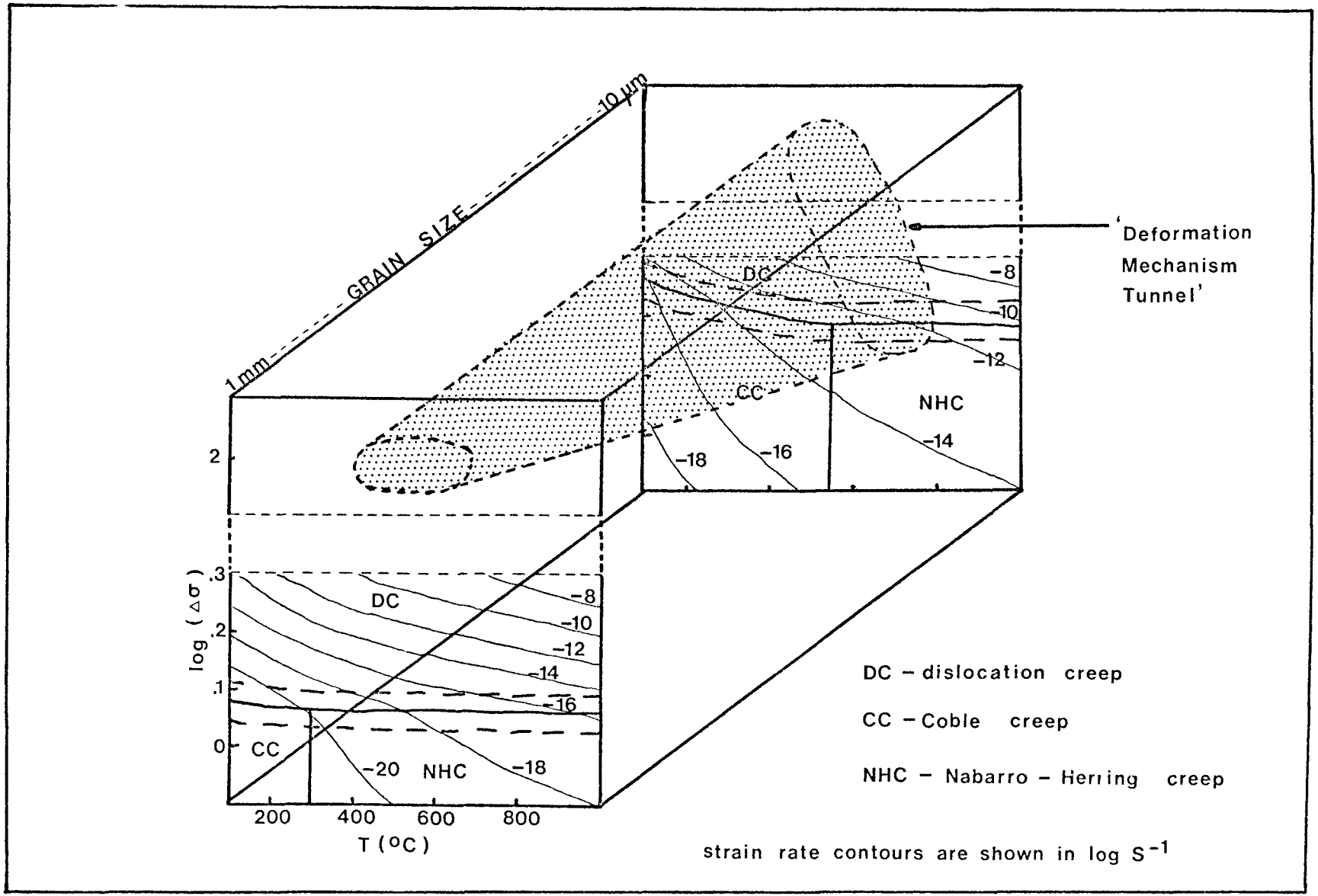

Deformation Mechanism Map for Sudbury Mylonites

(modified from White 1973)

Figure 9

DISCUSSION OF THE DEFORMATION MECHANISM MAP

A deformation map for grain sizes 1 mm to 10 μm is presented in Figure 9. The grain sizes refer to the mean grain size of the quartzite and to the pervasive matrix in a quartz mylonite. The boundaries between fields mark the position where two processes produce equal strain rates (White, 1973). The broken line on either side of the dislocation creep and diffusion creep boundary mark overlaps of one order of magnitude in strain rate.

The assumptions made in the construction of the maps coupled with the lack of accurate data in regard to differential stress, strain rate, and temperature restrict these maps to no more than "ball-park" accuracy. The maps do show that the diffusion creep field expands at the expense of dislocation creep with a reduction in grain size. Therefore, Nabarro-Herring creep may become a dominant deformation mechanism operating in the matrix of the mylonites. In addition, the map predicts that dislocation creep mechanisms such as climb and glide are the dominant deformation processes for quartzites with a grain size greater than 100 μm. This prediction is supported by the ubiquity of optical strain features observed in the rocks during the petrographic study. It also predicts a change in deformation mechanisms for grain sizes much less than 100 μm and that fine-grained quartz mylonites will deform under similar conditions much faster than coarser-grained mylonites.

CONCLUSIONS

(1) The Wanapitei quartzite in the Coniston study area shows a progressive increase in mylonitization from crush breccia to ultramylonite as the fault system is approached.

(2) The mylonites were produced by either pure shear or simple shear and essentially plot along the line k = 1 on the deformation plot. $\overline{k}$ for all the samples was calculated as 0.985. This indicates a constant volume deformation, as the samples plot between constriction-type deformation and flattening-type deformation.

(3) As the degree of mylonitization of the rocks increases, there are observed increases in the intensity of the undulatory extinction, subgrain development and the occurrence of deformation lamellae in the quartz grains.

(4) X-ray diffraction evidence indicates that the (100) plane of quartz becomes more oriented in the plane of foliation of the rock, due to recrystallization processes, as the Wanapitei fault is approached.

(5) Optically observed features such as undulatory extinction, deformation lamellae, and subgrain development can be explained in terms of dislocation movements and recrystallization and recovery processes.

(6) The deformation map indicates that dislocation climb and glide (dislocation creep) are the domination mechanisms operating in quartzites with a grain size > 100 μm. In addition, the diffusion creep field expands at the expense of dislocation creep with a

reduction in grain size. It is therefore possible that Nabarro-Herring creep may become a dominant deformation mechanism operating in quartz matrices with grain sizes of 10 μm or less.

REFERENCES

Belliere, J., 1971, Mylonites, Blastomylonites, et Domaines Polymetamorphiques, Ann. Soc. Geol. Belg., 94, pp. 249-263.

Bell, T.H., and M.A. Ethridge, 1973, Microstructure of Mylonites and Their Descriptive Terminology, Lithos 6, pp. 337-348.

Brace, W.F., B.W. Paulding and C. Scholz, 1966, Dilatancy in the Fracture of Crystalline Rocks, Jour. Geophys. Res., 71, pp. 3939-3954.

Card, K.D., 1968, Geology of the Denison-Waters Area, Ontario Dept. Mines Geol. Report 60.

Cooke, H.C., 1946, Problems of Sudbury Geology, Geol. Surv. Can. Bull. No. 3.

Dalziel, I.W.D., J.M. Brown and T.E. Warren, 1969, The Structural and Metamorphic History of the Rocks Adjacent to the Grenville Front near Sudbury, Ontario and Mount Wright, Quebec, Geol. Assn. Can. Spec. Paper 5, pp. 207-224.

Flinn, D., 1962, On Folding During Three-Dimensional Progressive Deformation, Quart. Jour. Geol. Soc. London 118, pp. 385-433.

Flinn, D., 1956, On the Deformation of the Funzie Conglomerate, Fetlar, Shetland, Jour. Geol. 64, pp. 491-527.

Friedman, M., 1975, Fracture in Rocks, Rev. Geophys. Space Phys., 13, pp. 352-358.

Grant, J.A., W.J. Pearson, T.C. Phemister, and Jas. E. Thomson, Broder, Dill, Neelon and Dryden Townships, Ontario Dept. Mines Report 9, 1962.

Handin, J., 1966, Strength and Ductility of Rocks, in S.P. Clark, Ed., Geol. Soc. Amer. Memoir 97, pp. 223-290.

Henderson, J.R., 1967, The Grenville Front in the Region East and South of Sudbury, Ontario, in Jenness, S.E., Geology of Parts of Eastern Ontario and Western Quebec, Guidebook, Geol. Assoc. - Can. Min. Assoc. Can., pp. 5-9.

Higgins, M.W., 1971, Cataclastic Rocks, U.S.G.S. Prof. Paper 687, pp. 1-97.

Hsu, Mao, Yang, 1968, Structural Analysis Along the Grenville Front near Sudbury, Ontario, unpublished M.Sc. Thesis, McMaster University, 104 pages.

Johnston, W.G.Q., 1954, Geology of the Temiskaming-Grenville Contact Southeast of Lake Timagami, Northern Ontario, Canada, G.S.A. Bull. V. 65, pp. 1047-1074.

Klug, H.P., and L.E. Alexander, X-Ray Diffraction Procedures for Polycrystalline and Amorphous Materials, John Wiley and Sons, New York, 1954, 716 pages.

Krupicka, A. and Sassano, G.P., 1972, Multiple Deformation of Crystalline Rocks in the Tazin Group, Eldorado Fat Mine, N.W. Saskatchewan, C.J.E.S. 9, pp. 422-434.

Kwak, T.A.P., Metamorphic Petrology and Geochemistry Across the Grenville Province - Southern Province Boundary, Dill Township, Sudbury, Ontario, Unpublished Ph.D. Thesis, McMaster University.

Oatley, C.W., The Scanning Electron Microscope, Cambridge Press, 1972, 194 pages.

Paterson, M.S., 1969, The Ductility of Rocks, in Physics of Strength and Plasticity, A.S. Argon, Ed., M.I.T. Press, Cambridge, Mass., pp. 377-392.

Paterson, M.S., 1970, Experimental Deformation of Minerals and Rocks Under Pressure, in The Mechanical Behavior of Materials under Pressure, H.D. Pugh, Ed., Elsevier Publishing Co., England, pp. 191-235.

Phemister, T.C., 1961, The Boundary between the Timiskaming and Grenville Subprovinces in the Townships of Neelon, Dryden, Dill and Broder, District of Sudbury, Ontario Dept. Mines, Prelim. Report 5, 1961.

Spry, A., Metamorphic Textures, Permagon Press, London, 1969, 350 pages.

Stocker, R.L. and M.F. Ashby, 1973, on The Rheology of the Upper Mantle, Rev. Geophys. Space Phys. 11, pp. 391-426.

Stockwell, C.H., 1964, Age Determinations and Geologic Studies, Geol. Surv. Can. Paper 64-17, Part 11.

Thomson, Jas. E., 1957, Geology of Falconbridge Township, Ontario Dept. Mines, Vol. 66, Part 6.

Tullis, J., Mylonites - Natural and Experimental, G.S.A. Short Course, March, 1978, Boston, Massachusetts.

Tullis, J. and R.A. Yund, 1977, Experimental Deformation of Dry Westerly Granite, Jour. Geophys. Res. 82, pp. 5705-5718.

White, S., 1973, The Dislocation Structures Responsible for the Optical Effects in Some Naturally Deformed Quartzes, Jour. Mat. Sci. 8, pp. 490-499.

White, S., 1976, The Effects of Strain on the Microstructures, Fabrics, and Deformation Mechanisms in Quartzites, Phil. Trans. Roy. Soc. London, 283, pp. 69-86.

Yates, A.B., 1968, Properties of International Nickel Company of Canada, in Structural Geology of Canadian Ore Deposits, Part 7, C.I.M.M., pp. 596-617.

Young, G.M. and W.R. Church, 1966, The Huronian System in the Sudbury District and Adjoining Areas of Ontario, Proc. Geol. Assoc. Can., Vol. 17, pp. 65-82.